



**ACCESS**  
Arctic Climate Change  
Economy and Society



**Project no. 265863**

# **ACCESS**

## **Arctic Climate Change, Economy and Society**

Instrument: Collaborative Project  
Thematic Priority: Ocean.2010-1 "Quantification of climate change impacts on economic sectors in the Arctic"

### **D4.44 – Report on oil flow under ice**

**Tor Nordam, CJ Beegle-Krause, Mark Reed**

Due date of deliverable: **30/09/2014**

Actual submission date: **13/03/2015**

Start date of project: **March 1<sup>st</sup>, 2011**

Duration: **48 months**

Organisation name of lead contractor for this deliverable: **SINTEF**

<b>Project co-funded by the European Commission within the Seventh Framework Programme (2007-2013)</b>		
<b>Dissemination Level</b>		
<b>PU</b>	Public	X
<b>PP</b>	Restricted to other programme participants (including the Commission Services)	
<b>RE</b>	Restricted to a group specified by the consortium (including the Commission Services)	
<b>CO</b>	Confidential, only for members of the consortium (including the Commission Services)	

## Contents

<b>Abstract</b>	<b>3</b>
<b>1 Background</b>	<b>4</b>
1.1 Oil Spill Contingency And Response Model (OSCAR) . . . . .	4
1.2 Input to the OSCAR model . . . . .	4
1.2.1 Environmental data . . . . .	5
1.2.2 Oil properties . . . . .	5
1.3 SINMOD Coupled Ice-Ocean Model . . . . .	6
1.3.1 Model set-up . . . . .	6
1.3.2 Atmospheric forcing . . . . .	7
1.3.3 Data produced . . . . .	7
<b>2 Scenarios and locations</b>	<b>8</b>
2.1 Scenario 1: Well Blowout, Coastal Greenland . . . . .	8
2.2 Scenario 2: Shipping Accident, Kara Strait . . . . .	10
2.3 Scenario 3: Pipeline Rupture, Varandey . . . . .	12
<b>3 Explanation of OSCAR model results</b>	<b>14</b>
3.1 Simulation results: Deterministic . . . . .	14
3.2 Simulation results: Stochastic . . . . .	16
3.3 Computational resources . . . . .	17
<b>4 Ensemble simulation results</b>	<b>17</b>
4.1 Scenario 1: Well Blowout, Coastal Greenland . . . . .	17
4.2 Scenario 2: Shipping Accident, Kara Strait . . . . .	24
4.3 Scenario 3: Pipeline Rupture . . . . .	30
<b>5 Conclusions</b>	<b>36</b>

## Abstract

Oil spills are of concern to coastal communities, decision makers and the Public. The threat of an oil spill and subsequent environmental and socio-economic effects are of more concern in the remote areas and under the harsher weather conditions of the Arctic. Most experience with oil spills has been in areas without significant ice cover because oil development and shipping are primarily located away from ice-covered waters. When oil prices are high, there is more incentive to move into more challenging areas, such as the Arctic. We have over the last few years seen a trend for shipping and oil development to move farther north. Because wildlife both migrate to the Arctic to feed in summer, such as whales, as well as to reproduce in compact colonies, such as birds, we have more potential for high wildlife impacts in areas of congregation

The distribution of oil and environmental risk caused by oil spills changes dramatically with the addition of ice. In open water, oil freely moves with the winds and currents. With higher ice cover, the ice increasingly contains and controls the movement of the oil. Oil movement transitions from just wind drift to the resultant of the wind and the ice drift at about 30% ice cover, and then to being controlled by the ice at about 70%. Spreading and weathering is known to reduce in high ice cover, allowing response options such as dispersant application or *in situ* burning to remain effective longer. We aim to answer the questions of how the fate of released oil changes between conditions today and future conditions with higher temperatures and less ice cover.

We have simulated three types of spills: a subsurface oil well blowout, a tanker accident, and a submerged pipeline leak. For each of the three scenarios, 698 simulations were performed, half in the period 2009-2013 and half during 2050-2054. This allows us to obtain statistics describing how the fate of released oil in an “average oil spill” will differ between the present, and the presumably warmer climate of the future. As expected, the presence of ice restricts the spreading of oil, particularly reducing the overall footprint of the spill at the surface.

Our results show that the length of oiled shoreline for the well blowout scenario is found to be almost twice as large in the future scenarios, while for the pipeline rupture and the tanker accident the amount of oil on the shore is slightly higher in the present, although there is little or no change in the length of oiled shoreline. For the well blowout scenario, we also see a significant increase in the amount of oil in the sediment in the future scenarios, and in general we see that in the future scenarios, the oil spreads further, reaching areas that were unaffected in the simulations under present conditions.

## 1 Background

Oil spills models commonly use ocean circulation data, wind and ice from other models as input. In this section, we describe the OSCAR model, used to carry out the simulations presented in this study, as well as SINMOD, which was used to produce the ocean circulation and the ice fields. The source of wind data, and the climate forecasts, are also discussed.

### 1.1 Oil Spill Contingency And Response Model (OSCAR)

OSCAR is a state of the art oil spill trajectory model for predicting the fate and effects of released oil, for example from a platform, a pipeline or a vessel. The model accounts for weathering, the physical and chemical processes affecting oil at sea, as well as biodegradation. The development of models for these processes is strongly coupled with laboratory and field activities at SINTEF on fate and effects of oil.

Subsurface oil well blowouts in OSCAR use a near-field model which includes a multiphase integral plume model [1, 2]. This model incorporates the buoyancy effects of oil and gas, hydrocarbon dissolution, hydrate formation, gas expansion and also includes the effects of the ambient water stratification, and cross flow on the dilution and rise time of the plume. Droplet size distribution due to turbulent break-up near the plume outlet is predicted using a model developed by Johansen *et al.* in 2013 [3, 4], accounting for interfacial tension between oil and water, oil viscosity, flow rate and outlet dimensions.

The OSCAR model computes surface spreading of oil, slick transport, entrainment into the water column, evaporation, emulsification and shore interactions to determine oil drift and fate at the surface. In the water column, horizontal and vertical transport by currents, dissolution, adsorption, settling and biodegradation are simulated. The varying solubility, volatility, and aquatic toxicity of oil components are accounted for by representing oil in terms of 25 pseudo-components [5], which represent groups of chemicals with similar physical and chemical properties. By modelling the fate of individual pseudo-components, changes in oil composition due to evaporation, dissolution and biodegradation are accounted for in the toxicity of the dissolved oil fraction. There is a biodegradation rate for each of the pseudo-components for the dissolved water fraction, droplet water fraction, surface and sediments.

The OSCAR model uses a pseudo-Lagrangian model where each model particle is tracked through the flow field, which is calculated from currents, wind (and ice if relevant). Buoyancy and sinking of oil droplets due to density differences or oil mineral aggregates are also included.

OSCAR has been involved in and is still in use for contingency planning, hind- and forecasting of accidental releases in locations such as the North Sea, Barents Sea, Gulf of Mexico and the Mediterranean Sea. OSCAR is continuously updated and actively developed in cooperation with the public and private enterprises, in order to improve the existing model and to be able to apply the model software to new challenges.

### 1.2 Input to the OSCAR model

The results of an OSCAR simulation is highly dependent on the various inputs to the model. Below, we give a brief description of the most important input parameters.

### 1.2.1 Environmental data

OSCAR uses data from an ocean circulation model as input. The currents should have a temporal resolution which is good enough to capture tidal effects, as these are important for shoreline interactions. For subsurface releases, a three-dimensional current field with good vertical resolution is also important.

Temperature and salinity can also be very important for correct calculation of velocity fields for transport in the ocean. The pycnocline, i.e., the layer where the density gradient is largest, will to some degree slow vertical transport, though oil can of course still rise through this layer due to most oils generally having lower density than even the least dense (low salinity, high temperature) water. Oils that sink in fresh water are not found in the Arctic. In addition to transport, the temperature is also important for calculation of evaporation.

The temperature and salinity at a given location, when presented as a function of depth, is known as a temperature or salinity profile, or T,S profile. Examples of temperature and salinity profiles are shown in Figures 1 and 2. These data are taken from the climate data set described in Section 1.3, which was generated by SINMOD. The geographical location the profiles are taken from is nearby the release point used in Scenario 1. Note that a fixed freezing temperature of  $-1.8^{\circ}\text{C}$  (independent of salinity) was used in the generation of the data.

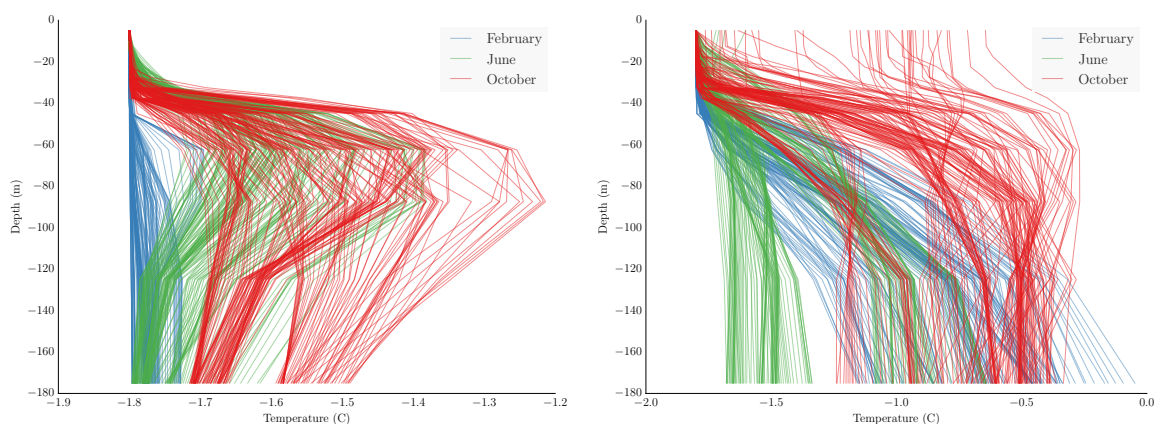


Figure 1: Daily temperature profiles for the location 10.0 W, 80.5 N (coastal Greenland), for the months of February, June and October. To the left, data for the years 2009 - 2013 are shown, to the right for the years 2050 - 2054. Note that the horizontal axes are different in the two plots.

### 1.2.2 Oil properties

The properties of the spilled oil are an important part of the input to OSCAR. The viscosity is important for correct determination of the oil slick properties, and the droplet size distribution in the event of a blowout, with droplet size distribution in turn determining what fraction the oil will surface, and when. Viscosity and chemical composition is also important in modelling the formation of emulsions. On the surface, a water-in-oil emulsion can form, which will have quite different properties from the pure oil. Chemical composition of the oil is also relevant for evaporation, and toxicity if impact is to be studied. Both the crude oils considered in this study have previously been characterised for use in OSCAR.

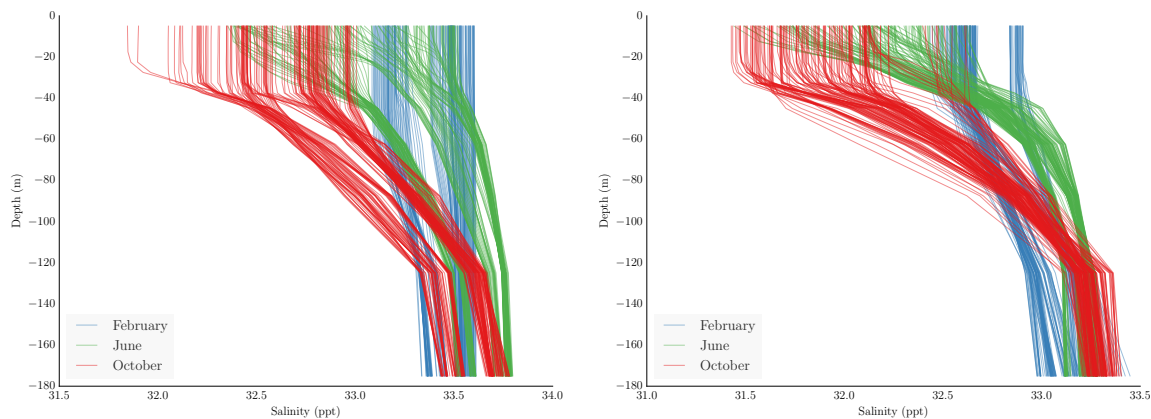


Figure 2: Daily salinity profiles for the location 10.0 W, 80.5 N (coastal Greenland), for the months of February, June and October. To the left, data for the years 2009 - 2013 are shown, to the right for the years 2050 - 2054. Note that the horizontal axes are different in the two plots.

### 1.3 SINMOD Coupled Ice-Ocean Model

Computer models of sea ice physics are generally coupled with ocean models in order to correctly simulate the freeze-melt cycle. Few are coupled atmosphere-ice-ocean models. Drozdowski *et al.* [6] reviewed sea ice models for use in oil spill trajectory calculations. The report indicates that regional scale coupled ocean sea ice models are most commonly used at climate scales of 10 to 100 km. As noted in the report, these models calculate an overall ice thickness and amount of open water in a grid cell, which can be converted into sea ice concentrations. These models are considered as “Hibler scheme” after Hibler [7], and are based on two key assumptions:

1. That the sea ice is continuous.
2. That the ice behaves as a viscoplastic material.

The SINMOD hydrodynamic model is based on the primitive Navier-Stokes equations and is established on a  $z$ -grid, using a constant-depth discretisation [8]. The vertical turbulent mixing coefficient is calculated as a function of the Richardson number,  $Ri$ , and the wave state. The flow becomes turbulent when  $Ri$  is smaller than 0.65 [9]. Near the surface, vertical mixing due to wind waves is calculated from wind speed and fetch length. Horizontal mixing is calculated according to Smagorinsky [10].

The ice model in SINMOD is a Hibler formulation [7], and has two state variables: average ice thickness,  $t$ , and ice compactness,  $A$ . The equation solver uses the elastic-viscous-plastic mechanism as described by Hunke and Dukowicz [11]. Ice compactness denotes the area fraction of a grid cell that is covered with ice, which is essentially the same as coverage. The remaining fraction,  $1 - A$ , is regarded as open water. Note that coverage is defined on the grid, so we only know the coverage for each  $4 \text{ km} \times 4 \text{ km}$  grid cell. No information about how the ice is distributed within each cell is available. In order to have a rough parameterisation of the porosity of the ice, the average freezing rate was introduced as an extra state variable.

#### 1.3.1 Model set-up

A new model set-up for a domain with 4 km grid resolution has been established. This set-up is nested into a larger domain having horizontal grid point distance of 20 km (see Figure 3). Simulation output from two periods, 2009-2013 and 2050-2054, have been produced. The initial

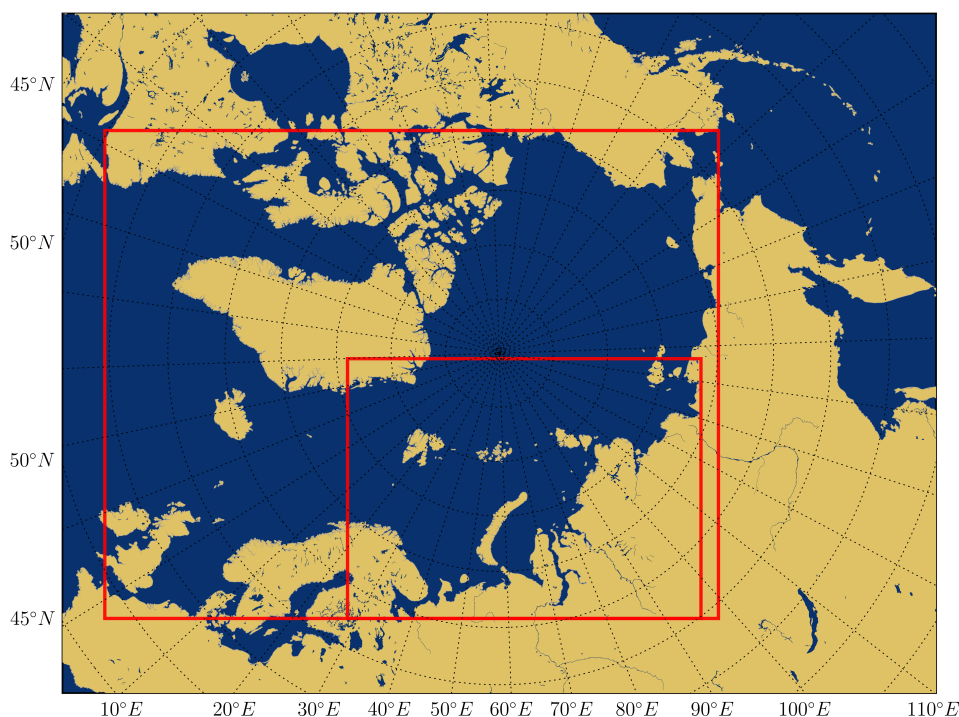


Figure 3: The extent of the 4 km × 4 km resolution SINMOD model area (small red rectangle), within the larger 20 km × 20 km resolution model area (large red rectangle). The 4 km × 4 km area was used to produce the data set used in this study.

values for the nested model domain are interpolated from the larger grid, allowing one year spin-up time. A total of 8 tidal components were imposed by specifying the various components at the open boundaries of the large-scale model. Data were taken from TPXO 6.2 model of global ocean tides [12].

The present set-up has 25 vertical levels. The levels which were modelled are the upper 10 m just below the sea surface, 10-15, 15-20, 20-25, 25-30, 30-35, 35-40, 40-50 m, then 50-75, 75-100, 100-150, 150-200, 200-250, 250-300, 300-400, 400-500, 500-700, 700-1000, 1000-1500, 1500-2000, 2000-2500, 2500-3000, 3000-3500, 3500-4000 and 4000-4500 m.

### 1.3.2 Atmospheric forcing

For the present climate simulation (2009-2013), the ERA-Interim Reanalysis [13] has been used. For the climate change case (2050-2054), the atmospheric forcing fields come from a regional model system run by the Max Planck Institute, REMO [14]. This model is configured to cover the model domain of SINMOD (Figure 3) and has a grid resolution of approximately 0.22°.

### 1.3.3 Data produced

The three-dimensional flow field and ice properties (ice velocity, under ice velocity, ice thickness, ice concentration and average freezing rate) were stored every 2 hours. The wind used as input to the hydrodynamic model was also stored every 2 hours, and on the same grid, for convenient use in the oil drift simulations. Hydrographic fields (temperature and salinity) were stored every 24 hours, as these change more slowly.

## 2 Scenarios and locations

Three scenarios were selected to be used as case studies:

1. A well blowout off the Northeast coast of Greenland
2. A pipeline rupture near Varandey Bay
3. A shipping accident in the Kara Strait

For each of these scenarios, over 600 simulations were performed, with the results presented in Section 4. A description and brief discussion of each scenario follows here. We would like to stress that these scenarios are fictitious, and were made up to show how the footprint of an oil spill might differ under a climate change scenario. These scenarios are not meant to represent the most likely oil spill scenarios in the Arctic, and do not take into expected changes in activities and shipping routes.

### 2.1 Scenario 1: Well Blowout, Coastal Greenland

Table 1: Scenario parameters for Scenario 1: well blowout off the coast of Greenland.

Location	10.9865 W, 80.8161 N
Release diameter	0.6604 m
Release rate	10000 metric tons per day
Release duration	50 days
Total release amount	500000 metric tons
Release depth	96 m
Sea depth at release location	97 m
Oil type	Statfjord C blend
Simulation duration	50 days

The first scenario is a well blowout, similar in flow rate and total amount released to the Deepwater Horizon event, in the Gulf of Mexico in 2010, although the area is much more shallow. The exact flow rate of that release is not known, with estimates ranging from around 2500 tons per day, up to 12500 tons per day [15]. In the well blowout simulations performed here, we have used a rate of 10000 metric tons per day, for 50 days, although modern permitting standards require that a capping stack must be available to be delivered in 5 days. The flow rate used can probably be said to be a high estimate for a well blowout at this location. The scenario could for example be loss of well control while drilling into a high pressure reservoir, capable of producing a high rate of unaided flow. For such a scenario, turbulence will break the release up into small droplets, with the droplet size distribution being dependent on, among other factors, oil viscosity, flow rate and release diameter. The release diameter has been chosen to be 0.6604 m (26 inches).

We have selected to use the properties of crude oil from the Statfjord C field for the modelling. The Statfjord C Blend crude oil is regarded as a paraffinic medium crude oil with a density of 0.834 g/mL (API gravity 38). The fresh oil has a medium content of wax (4.1 % by weight) and low asphaltenes (0.09 % by weight) compared with other crude oils in the Norwegian sector. The oil exhibits a medium evaporative loss and forms relatively stable water-in-oil emulsions with high water content (approximately 80 %).

In Figure 4 a map of the OSCAR model area is shown. The bathymetry is shown only down to 500 m in order for the details of the shallow areas to be more visible, but for the simulations

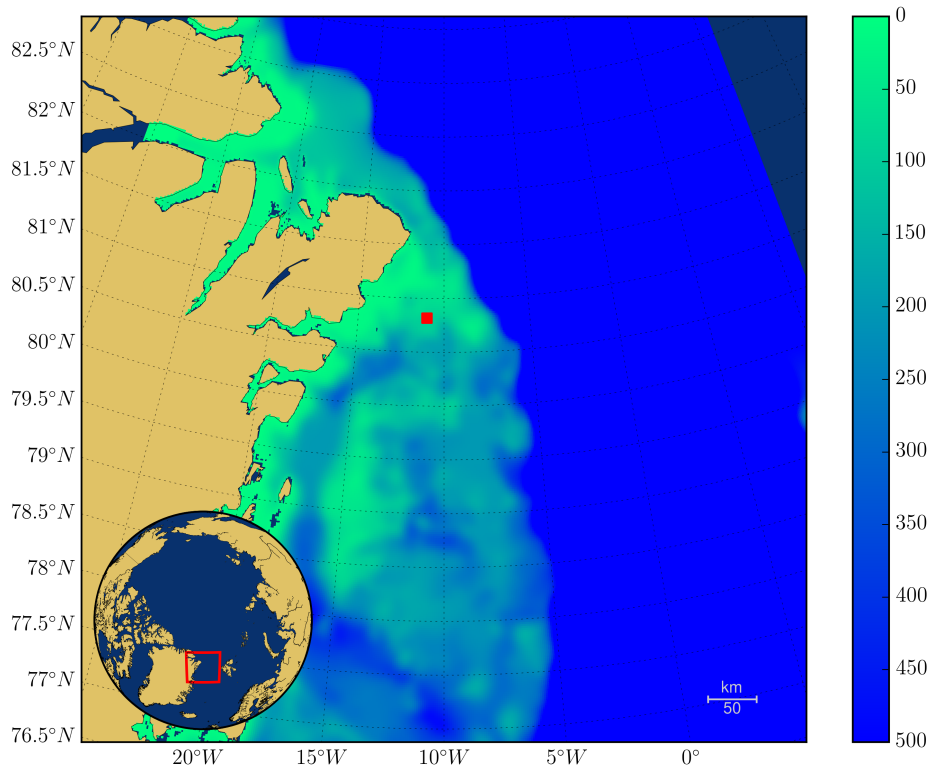


Figure 4: Model area for the well blowout simulations (Scenario 1), off the north east coast of Greenland. The bathymetry down to 500 m depth is shown, and the release point is marked by the red square. The rectangle on the inset globe shows the outline of the map.

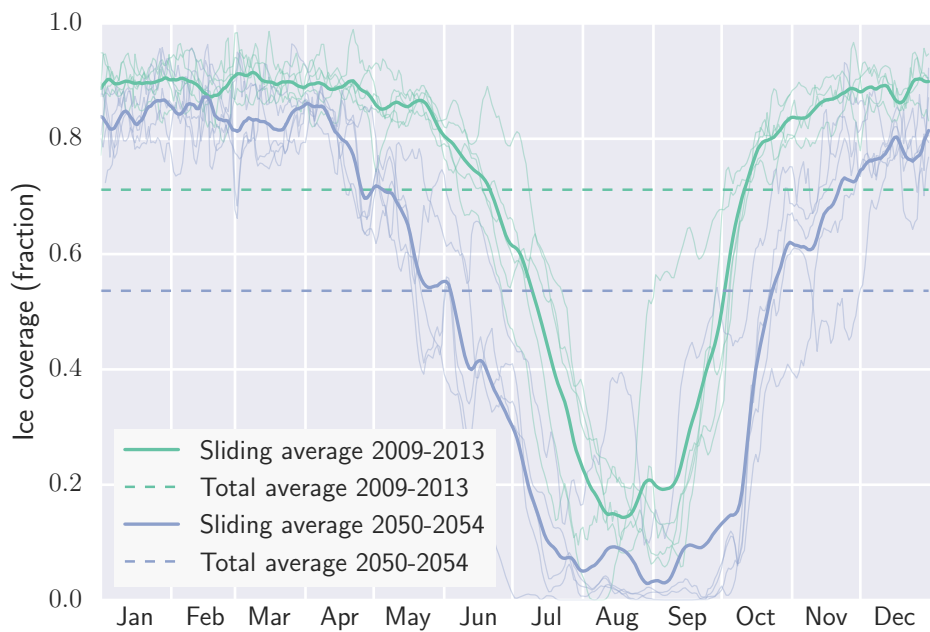


Figure 5: Ice coverage (fraction) in a 160 km × 160 km area centered on the release point. The thin lines show data for the individual years, the thick lines show a five-day sliding average of five years, and the dashed line show the total average over five years, with 2009-2013 shown in green and 2050-2054 shown in blue.

the full bathymetry was available to the model. Average ice coverage in an area around the release point is shown in Figure 5, with a comparison of present and future conditions. The most noticeable difference is that the open-water season is longer in the future. In the years 2009-2013, there are on average around 50 days with less than 30% ice coverage, while in the years 2050-2054, there are about 105 days with ice cover at less than 30%. At less than about 30% ice cover, oil moves as in open water. In the years 2009-2013, there are on average about 260 days with more than 70% ice cover, while for the years 2050-2054 there are about 180 days at higher than 70%. When the ice coverage is higher than about 70%, the movement of the oil is largely controlled by the ice, and spreading on the surface is strongly reduced.

A similar comparison was made for wind speed in the area, but showed no large difference from the years 2009-2013 to 2050-2054.

## 2.2 Scenario 2: Shipping Accident, Kara Strait

In this case, the scenario is a tanker accident in the Kara Strait, the strait between Novaya Zemlya and Vaygach Island, which separates the Kara Sea from the Barents Sea. The strait is quite narrow, about 55 km across, and quite shallow, around 50 meters at the deepest, and the currents can be quite strong, routinely reaching 1.5 m/s. The scenario assumes that a tanker leaks 40000 metric tons of crude oil over a period of 14 days, which could be due to a collision with another vessel or an iceberg, and the simulations are run for a total of 50 days. 40000 tons of oil can be said to be a “medium size” tanker accident. There have been a number of larger tanker accident spills, as well as a number of smaller ones. Compare for example to the *Exxon Valdez* spill, estimated at between 35000 and 110000 tons, and the *Prestige* spill at about 70000 tons. Tankers are expected to be larger in the future, though, so one might see a shift towards larger spills. A constant leak rate and a fixed position for the leaking vessel has been used in this scenario.

Table 2: Scenario parameters for Scenario 2: shipping accident in the Kara Strait.

Location	57.8862 E, 70.3296 N
Release rate	2857 metric tons per day
Release duration	14 days
Total release amount	40000 metric tons
Release depth	Surface release
Sea depth at release location	39 m
Oil type	Russian Crude
Simulation duration	50 days

The chosen oil, Russian crude oil (2010), is regarded as a paraffinic crude oil with a density of 0.856 g/ml (API gravity 33.7), with medium wax content (3.9 % by weight), and has a asphaltene content of 0.39 % by weight. The oil exhibits medium evaporative loss and forms stable water-in-oil emulsion (about 80% water content) after a short time of weathering at sea.

In Figure 6, a map of the model area is shown. The bathymetry is shown only down to 250 m in order for the details of the shallow areas to be more visible, but for the simulations the full bathymetry was available to the OSCAR model. Average ice coverage in an area around the release point is shown in Figure 7, with a comparison of present and future conditions. The most noticeable differences are that the open-water season is longer in the future, and that maximum ice cover during winter is lower for the future. In the years 2009-2013, there are on average around 180 days with less than 30% ice coverage, while in the years 2050-2054, there

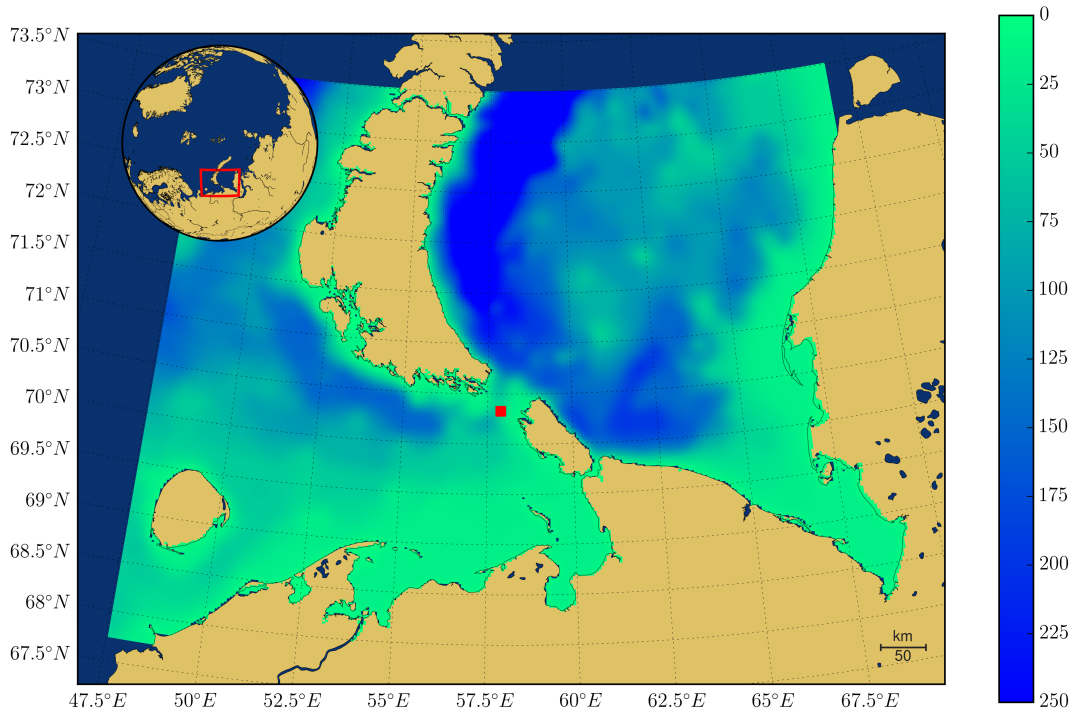


Figure 6: Model area for the shipping accident simulations (Scenario 2). The bathymetry down to 250 m depth is shown, and the release point is marked by the red square. The rectangle on the inset globe shows the outline of the map.

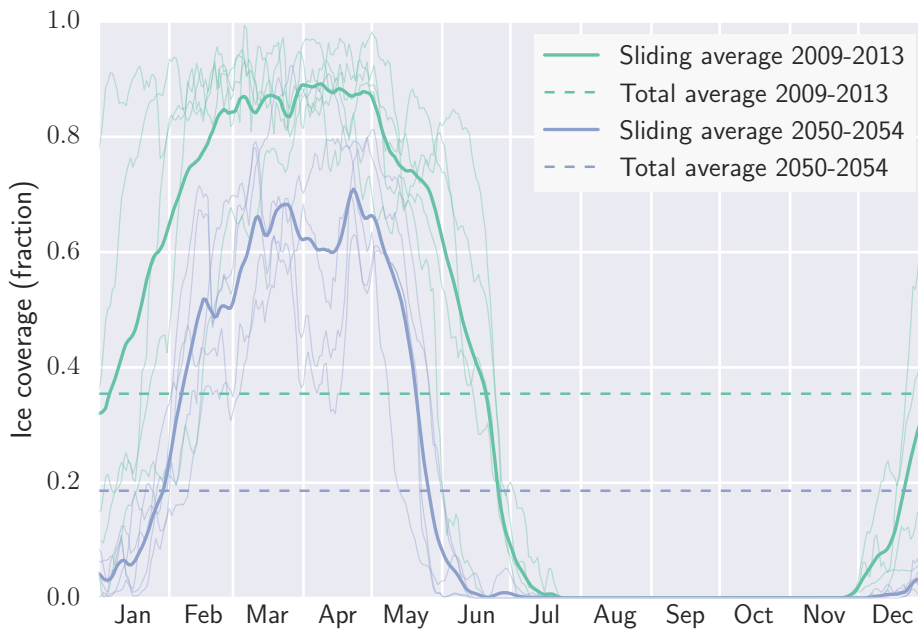


Figure 7: Ice coverage (fraction) in a 160 km × 160 km area centered on the release point. The thin lines show data for the individual years, the thick lines show a five-day sliding average of five years, and the dashed line show the total average over five years, with 2009-2013 shown in green and 2050-2054 shown in blue.

are about 260 days with ice cover at less than 30%. At less than around 30% ice cover, oil moves largely as in open water. Furthermore, during the years 2009-2013, there are on average around 100 days per year with ice cover higher than 70%, while for the years 2050-2054 the average year does not reach 70% ice cover.

A similar comparison was made for wind speed in the area, but showed no significant difference from the years 2009-2013 to 2050-2054.

### 2.3 Scenario 3: Pipeline Rupture, Varandey

The final scenario considered is a hypothetical oil spill from a pipeline leading to a loading terminal at sea. Such a pipeline could for example be damaged by gouging from an iceberg. We assume that a large leak in such a pipeline would be quickly detected, leading to only limited amounts of oil leaking out. In this scenario, a total of 416 metric tons (3000 barrels) have been assumed to leak from a position 1 m above the sea bed, over a period of 2 days. This is similar in magnitude to for example an oil spill from a pipeline (on land) in Arkansas in 2013, where an estimated 5000 barrels were released. The simulations have been run for 50 days, thus tracking the oil for an additional 48 days after the end of the release.

The selected oil, Russian crude oil, is the same as in Scenario 2. The oil is regarded as a paraffinic crude oil with a density of 0.856 g/ml (API gravity 33.7), with medium wax content (3.9 % by weight), and has a asphaltene content of 0.39 % by weight. The oil exhibits medium evaporative loss and forms stable water-in-oil emulsion (around 80% water content) after a short time of weathering at sea.

In Figure 8 a map of the model area is shown. The bathymetry is shown only down to 100 m in order for the details of the shallow areas to be more visible, but for the simulations the full bathymetry was available to the OSCAR model. Average ice coverage in an area around the release point is shown in Figure 9, with a comparison of present and future conditions. The conditions are naturally quite similar to those for Scenario 2, which is located nearby. Average ice cover is lower in the future, with the years 2009-2013 showing an average of around 100 days at above 70% ice cover, compared to around 20 days for the years 2050-2054. A similar comparison was made for wind speed in the area, but showed no significant difference from the years 2009-2013 to 2050-2054.

Table 3: Scenario parameters for Scenario 3: pipeline rupture near Varandey.

Location	57.8862 E, 69.0528 N
Release rate	208 metric tons per day
Release duration	2 days
Total release amount	416 metric tons
Release depth	16 m
Sea depth at release location	17 m
Oil type	Russian Crude
Simulation duration	50 days

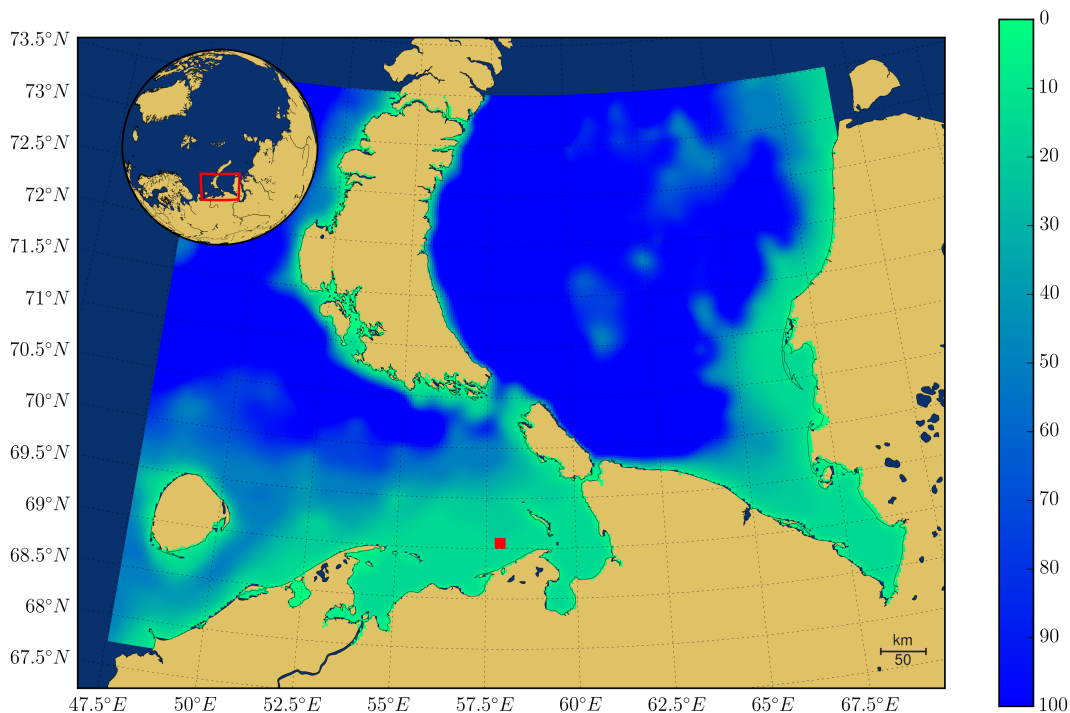


Figure 8: Model area for the pipeline rupture simulations (Scenario 3). The bathymetry down to 100 m depth is shown, and the release point is marked by the red square. The rectangle on the inset globe shows the outline of the map.

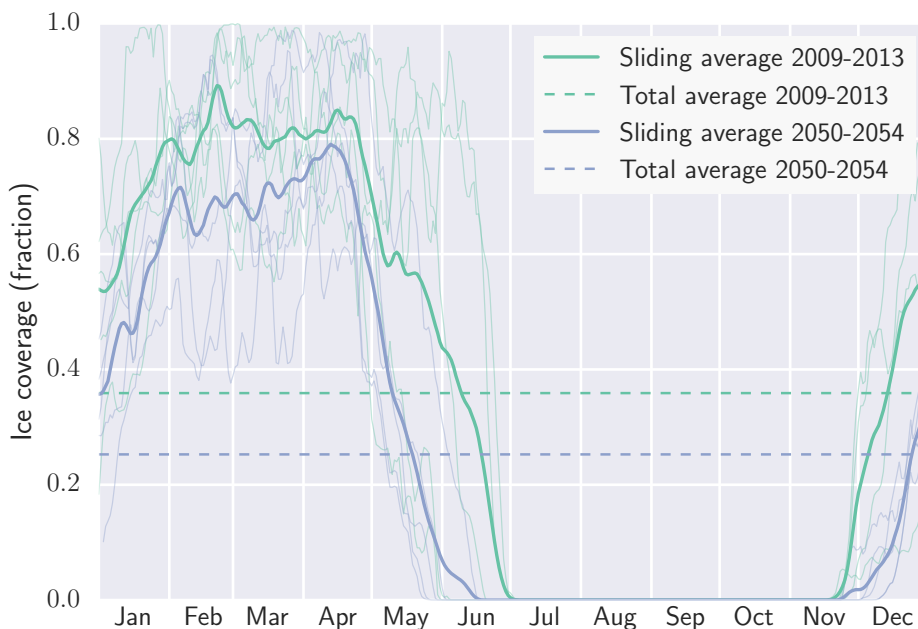


Figure 9: Ice coverage (fraction) in a 160 km × 160 km area centered on the release point. The thin lines show data for the individual years, the thick lines show a five-day sliding average of five years, and the dashed line show the total average over five years, with 2009-2013 shown in green and 2050-2054 shown in blue.

### 3 Explanation of OSCAR model results

In order to obtain statistical data about how the fate of released oil might differ due to warmer climate in the future, a large number of simulations was performed. Each individual simulation is frequently referred to as a “deterministic simulation”, because it is meant to provide the best possible answer to the question of what would actually happen if a given release scenario were to take place at the time and location specified.

For each of the three scenarios, one simulation was started every five days for the duration of the two five-year periods covered by the data set. This gives 698 simulations for each scenario, and provides a data set of oil spill behaviour and fate under varying met-ocean forcing. We can then analyse this data set, and obtain statistical information about the likely outcomes of a spill and the fate of the released oil.

#### 3.1 Simulation results: Deterministic

In this section, a short description of some examples of results that can be obtained from the OSCAR model is given. The results presented in this subsection are from deterministic simulations, i.e, simulations of single scenarios which represent a best estimate of what would actually happen if a release were to take place at a given place and time.

The simulation results from the OSCAR model include four dimensional  $(x, y, z, t)$  concentration fields giving concentration per component for droplets and dissolved chemicals, as well as three dimensional  $(x, y, t)$  grids for oil on the sea surface, on the shore and in the sediments. Additionally, some aggregated quantities are available as time series. These include amounts of evaporated oil, oil on the sea surface, submerged oil, oil on the shore, oil in the sediment and amount which has been biodegraded.

These last six quantities make up what is known as the mass balance, because it gives information about the fraction of the total mass which is found in any given “environmental compartment”. During the development of a spill, oil can move from one compartment to another. For example, oil on the surface can be mixed down by waves and submerged, submerged oil can resurface, stranded oil can be washed out to sea, etc. The exception is that oil which has been evaporated or biodegraded is removed from the simulation. Note that also oil which is trapped at the ice-water interface is considered to be at the surface in the mass balance calculation.

In open water conditions, wind can cause surface oil to be dispersed into the water column via wave action, and in shallow waters this vertical mixing can deposit oil in the sediments. Strong wind events can lead to relatively large changes in the mass balance over a short amount of time. An example is shown in Figure 10, which shows the mass balance during a simulation at two instants 36 hours apart. At the first time, there is around 40000 tons of oil submerged in the water column, and about 220000 tons on the surface. 36 hours later, there is 140000 tons of oil in the water column, and only 120000 tons on the surface. The extent of the surface slick for the same two instants is shown on a map in Figure 11.

The mass balance can also be presented as a time series for a single simulation. In Figure 12, an example of such a time series is shown. The data are presented in two ways, both as absolute numbers and as fraction of the released amount up to a given time. The data shown are from the same scenario as that shown in Figures 10 and 11. The large change in amount of submerged oil and oil on the surface is clearly visible around 42 days after the start of the simulation.

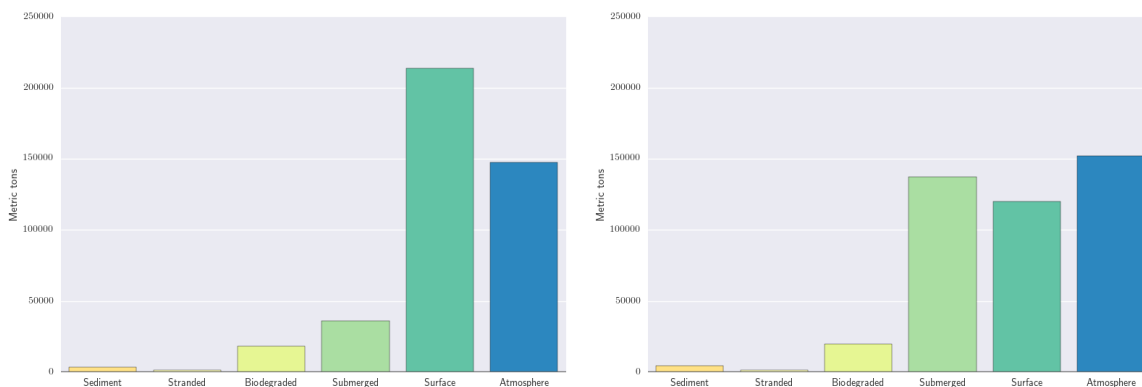


Figure 10: Mass balance for Scenario 1 (well blowout). The start date of the simulation was July 17 2012. To the left, the mass balance after 42 days is shown, and to the right after 43 days and 12 hours, after a strong wind event. Note the large change in amount on the surface and amount submerged. Strong wind can cause oil on the surface to be mixed down into the water column.

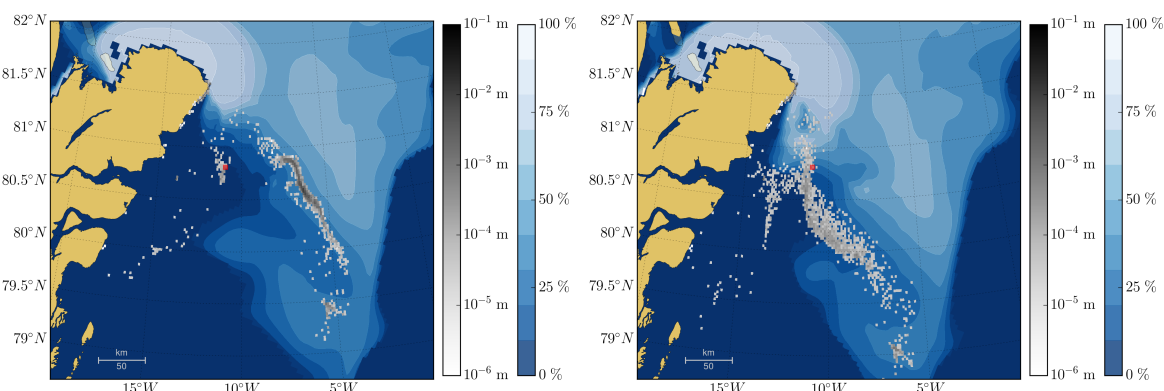


Figure 11: Distribution of surface oil for Scenario 1 (well blowout), with oil thickness shown in a white-to-black scale and ice coverage in a blue-to-white scale. The release site is marked by the red square. The start date of the simulation was July 17, 2012. To the left, the oil slick after 42 days is shown, and to the right after 43 days and 12 hours. Note the change in the extent and thickness of the slick.

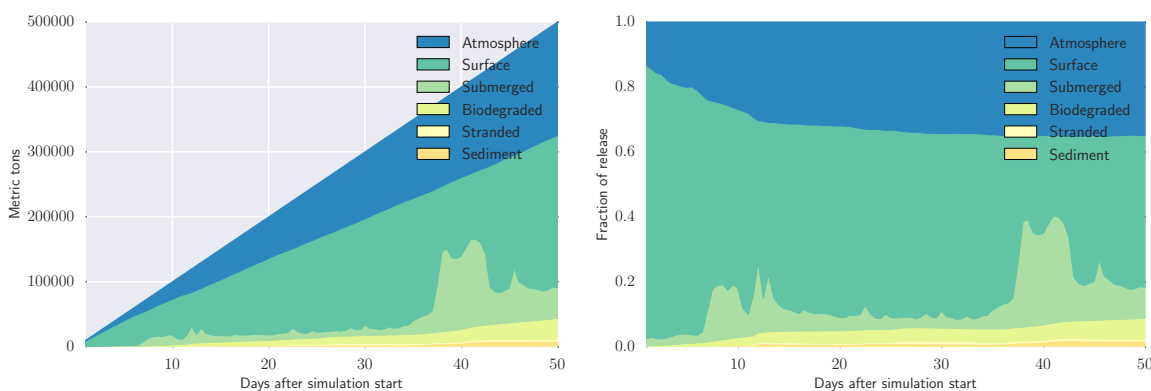


Figure 12: Mass balance as a function of time from simulation start, for Scenario 1. The start date of the simulation was July 17, 2012. To the left, the amount in tons is shown, to the right the fraction of the total released amount, in both cases showing the amount in each environmental compartment at each time.

### 3.2 Simulation results: Stochastic

Climate change and global warming do not necessarily mean that any given day, or any given year, will be warmer in the future, but rather that global average temperature will be higher. Thus, any given scenario by itself is not particularly interesting in the context of climate change. By performing a large number of simulations, spread out over both the two five-year periods for which data were available, we can generate statistical data and investigate how an “average oil spill” in the future will compare to one in the present. Note that each individual OSCAR simulation uses the full resolution of the current, wind and ice fields.

The procedure is essentially a form of Monte Carlo averaging, i.e., an average over an ensemble of simulations where at least part of the input is in some sense random. The environmental data which is given to the model as inputs, currents, winds, ice, temperature and salinity, are not independent, and it is not easy to generate random realisations of these fields which are still physically consistent. However, by using sequences of data taken from the two five-year datasets, we are sampling from the underlying probability distribution. It could probably be discussed whether some other sampling scheme than the regular intervals used here would be better. For example, when calculating averages based on all the samples, simulations which take place during calm weather are given equal weight as those which take place during adverse weather conditions. In reality, it could for example be more likely for a spill, at least one caused by a shipping accident, to take place during bad weather. Regular sampling was nevertheless chosen, because it is trivial to implement, easy to explain and it has the distinction of being commonly used in contingency analysis during planning of new activities.

For each of the three scenarios presented here, we have performed a 50-day simulation every 5 days for the duration of both the two five-year periods. Thus, if the first simulation had a start date of January 1, 2009, it would run until February 20, 2009. The next simulation would have a start date of January 6, 2009, and run until February 25, etc. These two simulations would then see partially different environmental data, with the difference in the results being highly dependent on the type of scenario.

For a well blowout (Scenario 1), the oil released during the 45 days the two simulations have in common would behave largely the same (some difference is possible, due to dissolution of soluble oil components being controlled by ambient concentration, which could differ). For a short release, on the other hand, such as the pipeline rupture (Scenario 3) studied here, the oil is released over a period of only two days, and then tracked for another 48 days as it is transported with winds and currents. For a scenario like this, the outcome can look completely different depending on what happens in the first five days, and two simulations partially overlapping in time might thus turn out very different from each other.

In Figure 13, the difference between two overlapping simulations is shown. To the left, a simulation with start date July 13, 2010 is shown, to the right with start date July 18, 2010. In both cases, the snapshot is taken on August 2, 2010. The pictures are taken from Scenario 1, which is a well blowout, so the only difference between the two pictures is made up by the extra five days of oil release in the picture to the left. Note the strong similarity between these plots. Obviously, when two non-overlapping scenarios are considered, the results are likely to look very different. By considering an ensemble of simulations with different start dates, it is possible to obtain statistical information on the likely outcome of an oil spill, and also to investigate how the likely outcome changes between seasons and between years.

It can furthermore be interesting to look at one of the compartments of the mass balance, for example the amount of oil on the surface, presented at the end of each 50 day simulation, as a

function of the start date of the simulation. An example of this is found in Figure 14, which shows the amount of oil on the surface. It is immediately clear that during summer, there is on average less oil on the surface than during winter. The reason for this is that high ice cover will prevent wind and waves from mixing the oil down into the water column. Not unexpectedly, we also see that the summer season is longer in the future. The average amount of oil on the surface at the end of each of the simulations for the period 2009-2013 is 302000 tons, while for the period 2050-2054 the average is 270000 tons. It is also worth observing that the change in total average from the present to the future is smaller than the variation between summer and winter.

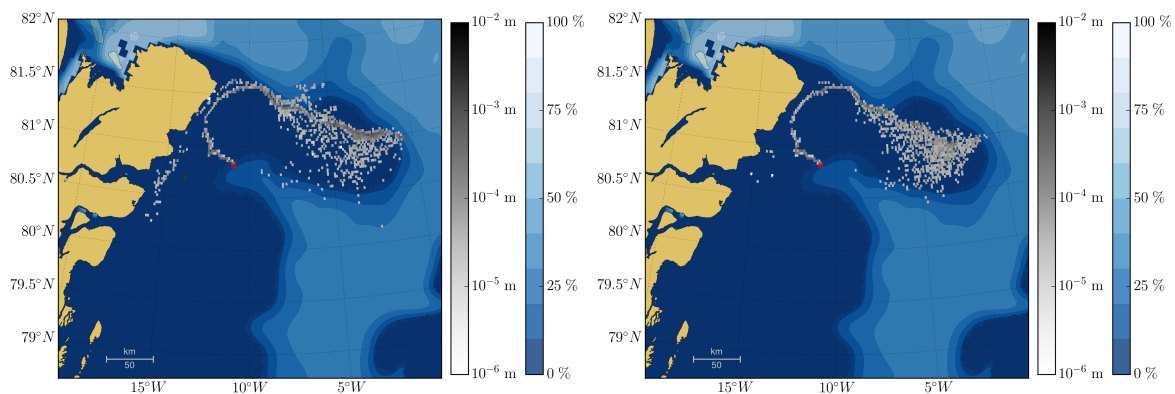


Figure 13: Distribution of surface oil for Scenario 1 (well blowout), with oil thickness shown in a white-to-black scale and ice coverage in a blue-to-white scale. The release site is marked by the red square. To the left, the start date of the simulation was July 13, 2010, to the right July 18, 2010. Both slicks are shown on August 2, 2010, which means that the only difference in the two figures is that the spill on the left started five days earlier. The similarities between the two plots are readily apparent. Subsequent scenarios will be increasingly different, as more of the simulation time is covered by different environmental data.

### 3.3 Computational resources

Following the procedure described above, we ended up running 698 simulations, half in the period 2009 - 2013 and half during 2050 - 2054, for each of the three scenarios. Depending on the scenario, one simulation takes about an hour to two and a half hours to complete, giving a total of about 150 days of CPU time. The simulations were for the most part performed on a 32-core compute node running linux, with 28 simulations running in parallel. The compute node was fitted with 10 TB of fast access disk space, allowing the entire environmental dataset to be kept on the node and used directly.

## 4 Ensemble simulation results

In this section, we will present and discuss the results of the ensemble simulations. The same results will be presented for each of the three scenarios, but as a number of general remarks and some trends apply to all three scenarios, the results from Scenario 1 will be treated in a bit more detail than the two others.

### 4.1 Scenario 1: Well Blowout, Coastal Greenland

In Figure 15 the quantity of oil at the surface, at the end of a 50 day simulation, with the scenario parameters presented in Table 1, is shown, as a function of start date of the simulation. There is

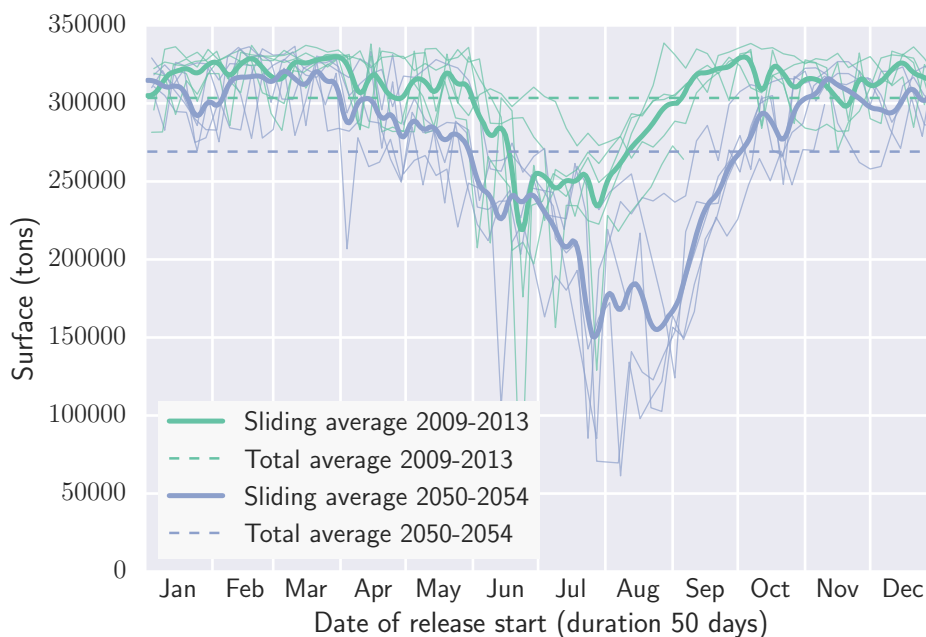


Figure 14: Amount (in metric tons) of oil on the surface, at the end of each 50 day simulation, shown as a function of start date for the simulation. The thin lines show data for the individual years, the thick lines show a five-day sliding average of five years, and the dashed line show the total average over five years, with 2009-2013 shown in green and 2050-2054 shown in blue.

a clear trend showing less oil on the surface during the summer months. Since oil typically has lower density than water, oil droplets will rise to the surface, and once at the surface will remain there unless wind and waves cause the oil to be mixed down. When there is ice cover, the effects of wind and waves are reduced or removed, meaning that oil which reaches the surface in full ice cover is more likely to remain at the surface. Note that surface oil here includes oil which is trapped at the water/ice interface. Due to a longer period of open water, there is on average less oil on the surface in the future scenarios. Furthermore, although the average is smaller in the future scenarios, the variability is higher, with a standard deviation of 36400 tons (12% of the average) in the present, and 57000 tons (21% of the average) in the future.

When comparing Figure 15 to Figure 5, which shows ice coverage as a function of date, the same trend of a longer summer season in the future is visible. The reason the figures appear shifted, with the low point for ice coverage both in the present and the future occurring at a later point than the low point for oil on the surface, is that the simulation results are shown at the end of each 50 day simulation, yet shown as a function of start date. This is the case for all figures showing simulation results as a function of start date.

In Figures 16 and 17, the area covered by thick oil (thickness greater than 100 µm) and the total oil covered area, are shown. On average, the slick covers a larger area in the future scenarios. This is expected from the discussion above. Oil which remains on the surface will tend to move as a slick. When the oil is dispersed into the water column, however, different droplet sizes will rise with different speeds. Smaller droplets will tend to stay submerged longer, while larger droplets will rise faster. Since the current near the surface often changes relatively quickly with depth, this leads to spreading over a larger area whenever oil is mixed down into the water column. The total averages are 556 km<sup>2</sup> of thick oil and 1780 km<sup>2</sup> of surface oil for 2009-2013 and 604 km<sup>2</sup> of thick oil and 4110 km<sup>2</sup> of surface oil for 2050-2054, meaning the surface slick is

on average more than twice as large in the future scenarios.

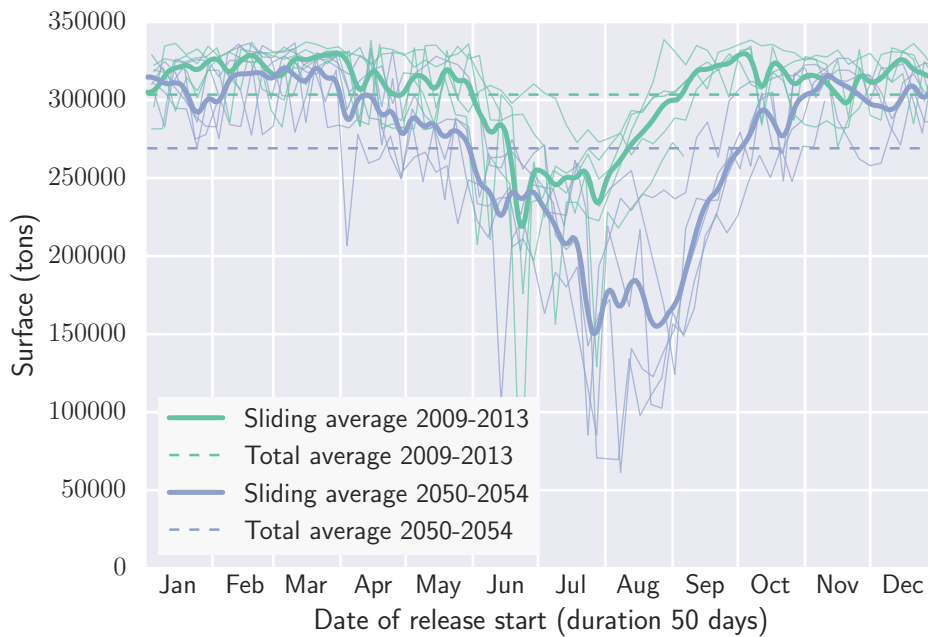


Figure 15: Amount (in metric tons) of oil on the surface, at the end of each 50 day simulation, shown as a function of start date for the simulation. The thin lines show data for the individual years, the thick lines show a five-day sliding average of five years and the dashed lines show the total average of five years, with 2009-2013 shown in green and 2050-2054 shown in blue.

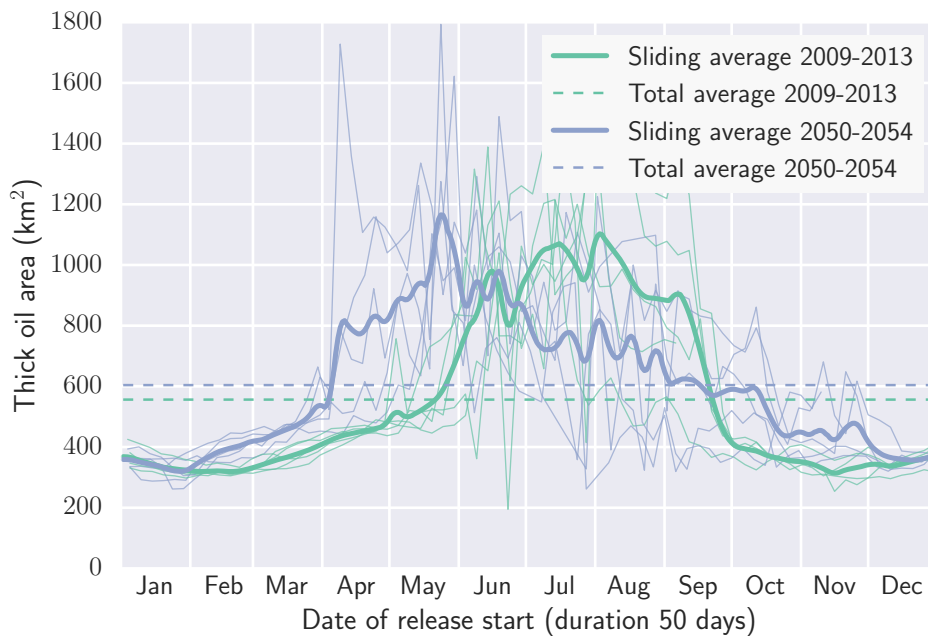


Figure 16: Area (in km<sup>2</sup>) covered by oil thicker than 100 μm, at the end of each 50 day simulation, shown as a function of start date for the simulation. The thin lines show data for the individual years, the thick lines show a five-day sliding average of five years and the dashed lines show the total average of five years, with 2009-2013 shown in green and 2050-2054 shown in blue.

The total amount of oil on the shore is shown in Figure 18, with the total length of shoreline

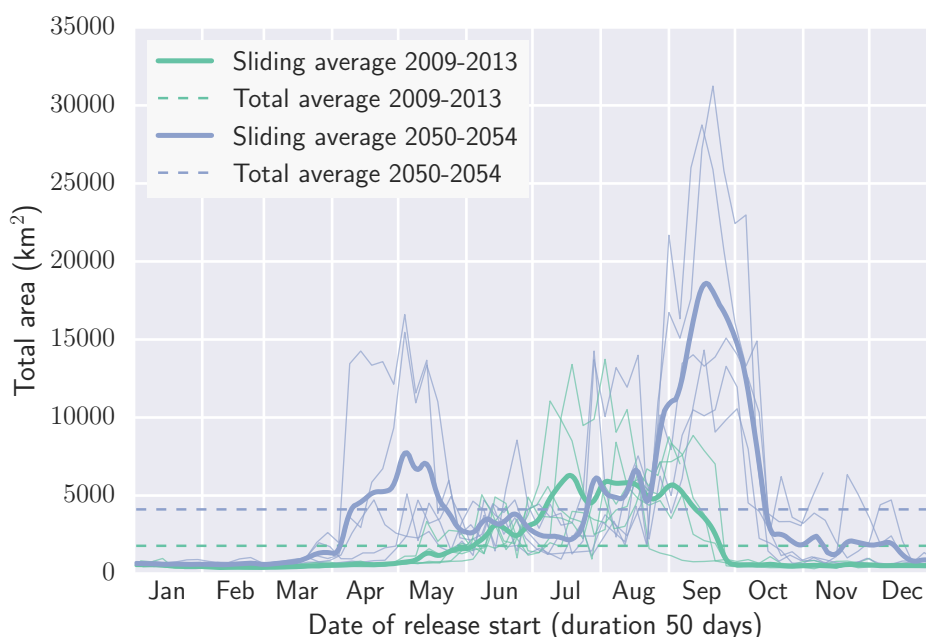


Figure 17: Area (in km<sup>2</sup>) covered by oil, at the end of each 50 day simulation, shown as a function of start date for the simulation. The thin lines show data for the individual years, the thick lines show a five-day sliding average of five years, and the dashed lines show the total average of five years, with 2009-2013 shown in green and 2050-2054 shown in blue.

affected by oil shown in Figure 19. For both of these endpoints, we see a quite significant increase in the average between the present and the future, with a total average of 1720 tons of stranded oil and 213 km of oiled shoreline for 2009-2013, compared to 4900 tons and 529 km for 2050-2054.

Climate change results in changes in the distribution of overall atmospheric pressure. Index measures of relative pressure such as the North Atlantic Oscillation (NAO), which is pressure difference between the Iceland Low and the Azores High, show changes in the overall pressure pattern in the North Atlantic related to climate change [16]. These changes lead to an intensification in storm activity in the Nordic seas due to northward shift in the storm tracks [17, 18, 19]. The change in storm tracks likely lead to the differences in beaching patterns in Northern Greenland between the two sets of simulations. Though we have not found research on climate change effects on weather systems in the Kara Sea, Woollings’ results [19] suggest that storm tracks in this area are not highly effected. This would explain the lack of changes in beaching in the pipeline and tanker scenarios under climate change (see Sections 4.2 and 4.3). Instead, we see only a lengthening of the summer period.

The amount of oil in the sediments is shown in Figure 20. Again, we see a marked increase in the future scenarios. When there is open water, strong winds can generate large, breaking waves which can mix the water column to a depth of 50 - 100 meters or more. Evidence of this mixing can also be seen in the temperature profiles shown in Figure 1, where the mixed layer (layer with near constant temperature) can be seen to be deeper in some of the future profiles. This mixing process can deposit oil in the sediments at these depths, while smaller waves can cause oil to end up in the sediments in more shallow waters. The total average over all the simulations is 3150 tons for 2009-2013, and 9740 tons for 2050-2054.

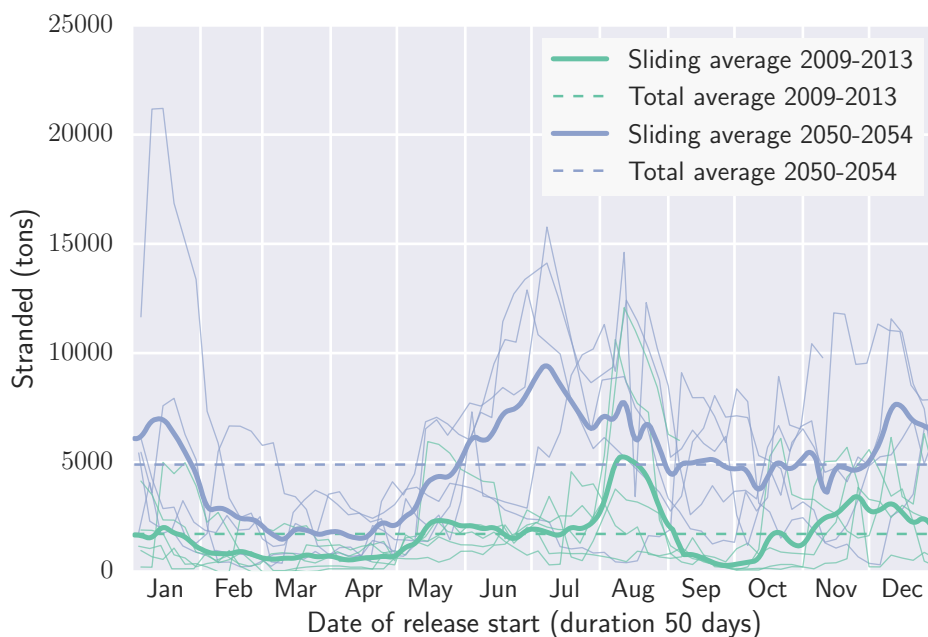


Figure 18: Amount (in metric tons) of oil on the shore, at the end of each 50 day simulation, shown as a function of start date for the simulation. The thin lines show data for the individual years, the thick lines show a five-day sliding average of five years, and the dashed lines show the total average of five years, with 2009-2013 shown in green and 2050-2054 shown in blue.

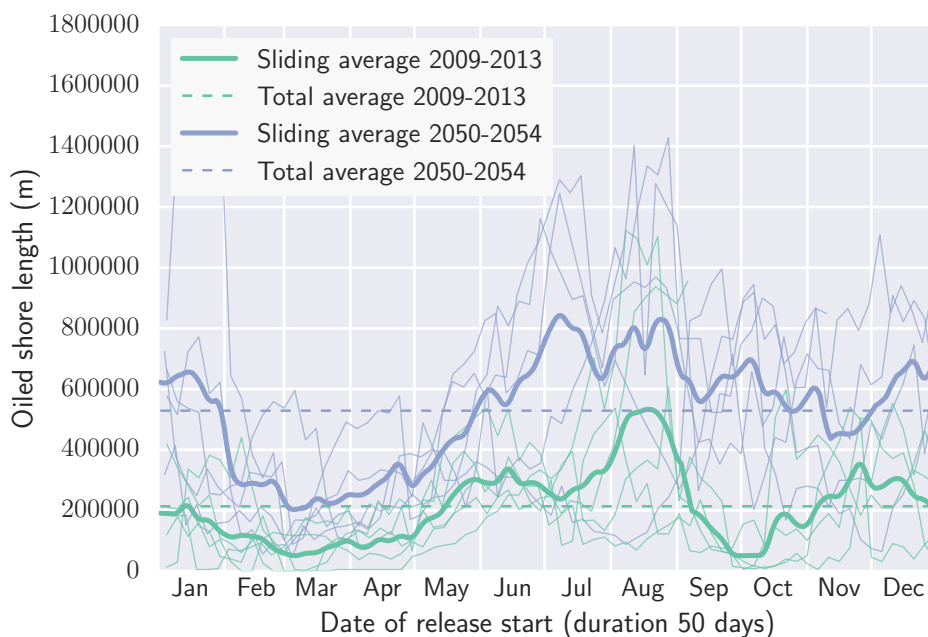


Figure 19: Length (in m) of shore affected by oil, at the end of each 50 day simulation, shown as a function of start date for the simulation. The thin lines show data for the individual years, the thick lines show a five-day sliding average of five years, and the dashed lines show the total average of five years, with 2009-2013 shown in green and 2050-2054 shown in blue.

All the results that have been presented as time series are also summarised in Table 4.

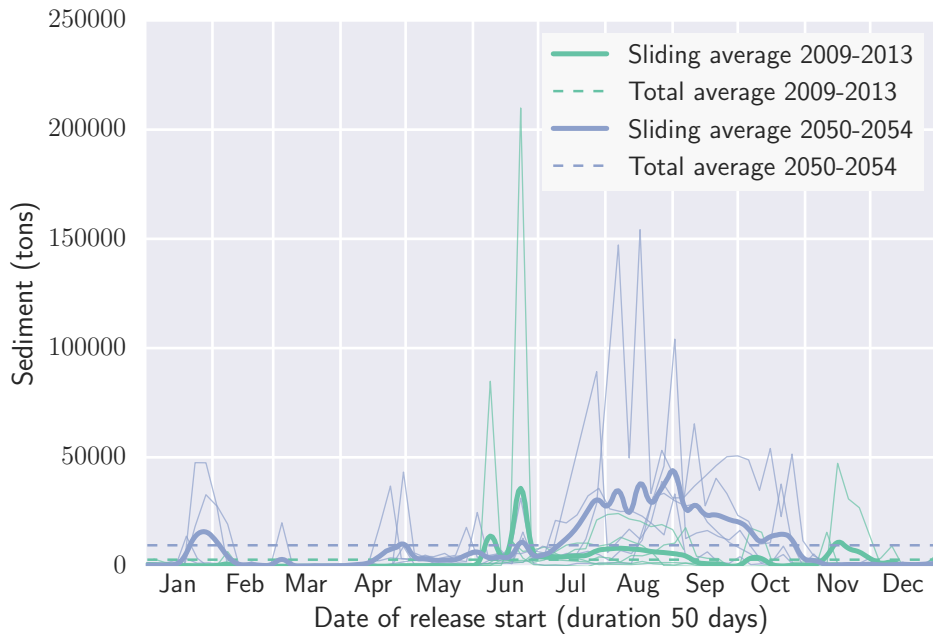


Figure 20: Amount (in metric tons) of oil in the sediments, at the end of each 50 day simulation, shown as a function of start date for the simulation. The thin lines show data for the individual years, the thick lines show a five-day sliding average of five years, and the dashed lines show the total average of five years, with 2009-2013 shown in green and 2050-2054 shown in blue.

The full mass balance is shown in Figure 21, with the years 2009-2013 on the left, and 2050-2054 on the right. As can be seen, the changes between the present and the future are relatively modest. The winter season is very similar in both cases, whereas the summer season is both longer and a bit warmer in the future. This is as expected, since in winter there is full ice cover both in the present and the future, whereas there is a longer season of open or partially open water in the future. During summer, there is a small increase in evaporation and biodegradation in the future, with a somewhat larger increase in amount in sediments and amount suspended in the water column. The amount of oil on the shore is also nearly double in the future scenarios compared to the present, although this makes up only a small fraction of the total release.

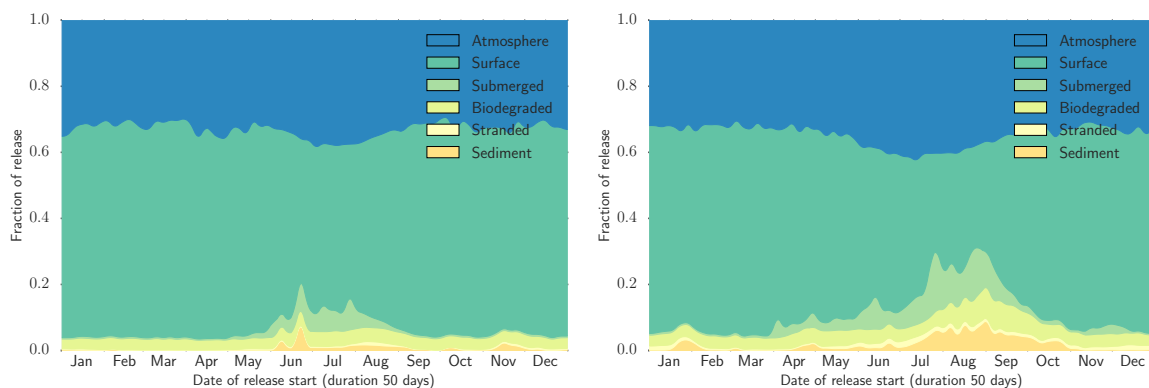


Figure 21: The full mass balance, at the end of each 50 day simulation, as a function of start date for the simulation and shown as a five-day sliding average over the five years. To the left, the years 2009 - 2013, to the right 2050 - 2054.

Table 4: Summary of results for Scenario 1: well blowout off the coast of Greenland.

	Present		Future	
	Average	Standard deviation	Average	Standard deviation
Total area (km <sup>2</sup> )	1840	2420	4250	5520
Thick oil area (km <sup>2</sup> )	566	310	606	282
Oiled shore length (m)	216000	200000	518000	324000
Sediment (tons)	3200	13200	9430	18100
Stranded (tons)	1730	1910	4750	3700
Biodegraded (tons)	17900	3790	23200	9500
Submerged (tons)	9170	16700	19200	28200
Surface (tons)	303000	36400	270000	57000
Atmosphere (tons)	165000	18800	173000	21900

In Figure 22, the maximum thickness of oil on the surface, at any point during all simulations, is shown for the years 2009-2013 on the left, and 2050-2054 on the right. In Figure 23, the expectation value of thickness of oil on the surface is shown. For any given point, the expectation value in that point is the sum of the thickness in that point over all output timesteps in all simulations, divided by the number of timesteps. The output timestep used was 6 hours for all three scenarios.

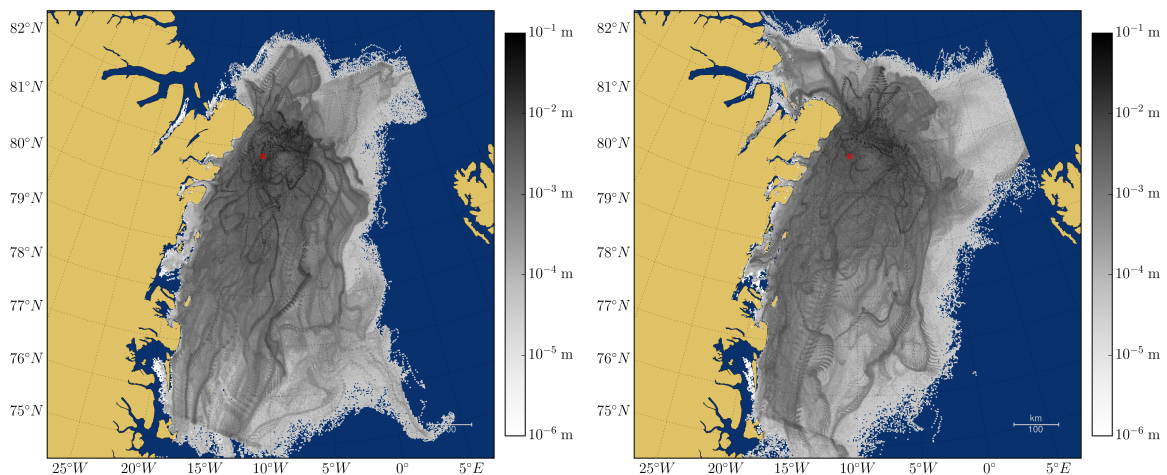


Figure 22: Maximum value of oil thickness on surface, over all simulations over the two five year periods. To the left 2009 - 2013, to the right 2050 - 2054. Only values larger than  $10^{-6}$  m is shown.

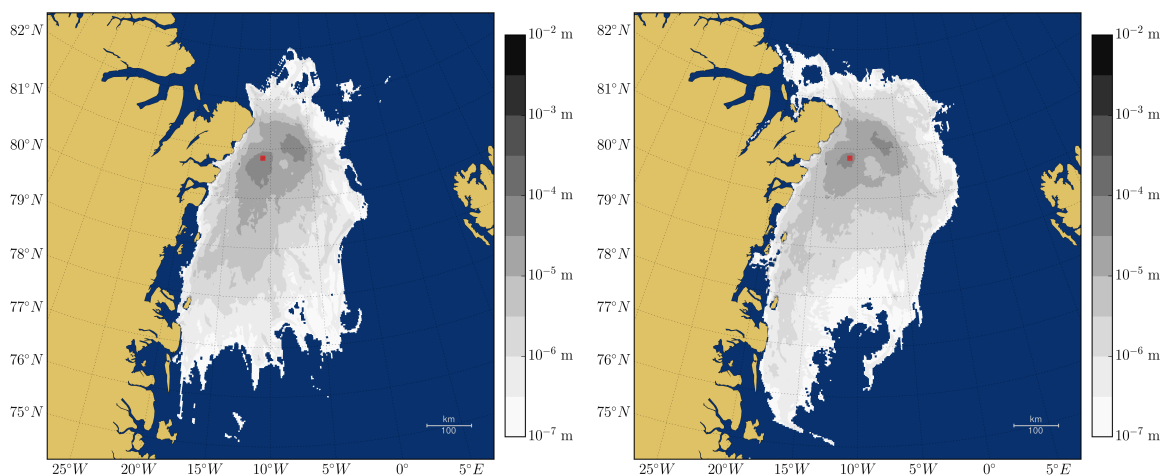


Figure 23: Expectation value of oil thickness on surface, over all simulations over the two five year periods. To the left 2009 - 2013, to the right 2050 - 2054. Only values larger than  $10^{-7}$  m is shown.

## 4.2 Scenario 2: Shipping Accident, Kara Strait

Many of the same observations that were made about the results of Scenario 1 (the well blowout) will apply to these results as well. Hence, the discussion here will be somewhat shorter, with more detailed comments where the results differ from what was seen previously.

In Figure 24, the amount of oil on the surface, at the end of each 50 day simulation, is shown as a function of start date of that simulation. The same general trend of less oil on the surface in the future scenarios is visible, although it is less pronounced. The total averages are 10200 tons for the present scenarios, and 7250 tons for the future.

The area covered by oil thicker than 100  $\mu\text{m}$ , and the total area covered by oil are shown in Figures 25 and 26 respectively. The trend of larger area covered in the future is visible here as well, although the difference in the total averages is modest: 12  $\text{km}^2$  (area with thick oil) and 895  $\text{km}^2$  (total area) for the present scenarios, versus 15  $\text{km}^2$  (area with thick oil) and 1100  $\text{km}^2$  (total area) for the future scenarios. Note, though, that from the thin lines showing the individual years in Figure 25, it can be seen that in some cases the area covered by thick oil can reach 150  $\text{km}^2$ , which is 10 times the average for the future scenarios. Under the right circumstances, this could almost certainly happen in the present scenarios as well. In any case, it serves to illustrate the dramatic difference that can be observed in two spills which are separated by a few days, but otherwise identical in all respects.

Figure 27 shows the length of oiled shoreline, and Figure 28 shows the amount of oil on the shore. In this case, the length of oil shoreline is essentially the same between now and the future, at 265 km and 261 km respectively. Amount of oil on the shore shows some difference, with 1460 tons at present, versus 1160 tons in the future scenarios. In other words, unlike what was seen for the well blowout, there is in this case *more* oil on the shore in the present scenarios. Comparing Figure 27 to the ice coverage for the area, shown in Figure 7, we see that in this case, there is on average more oil on the shore when ice coverage is high, although the correlation is not perfect.

The amount of oil in the sediments is shown in Figure 29. As expected, there is an increase in the amount that ends up in the sediment when ice cover is low. Due to the area being relatively shallow, with large areas at only a few tens of meters deep, a significant fraction of the release

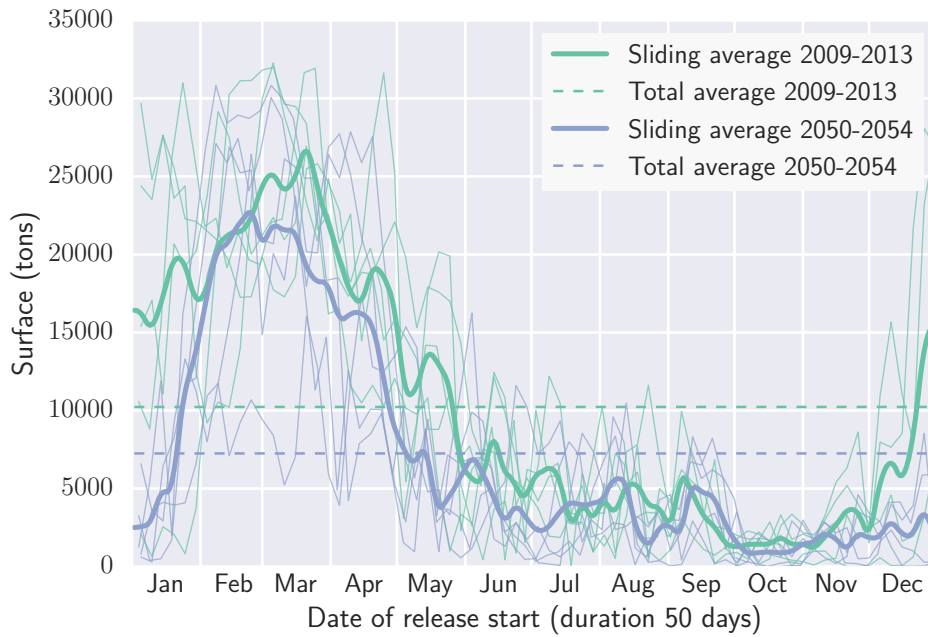


Figure 24: Amount (in metric tons) of oil on the surface, at the end of each 50 day simulation, shown as a function of start date for the simulation. The thin lines show data for the individual years, the thick lines show a five-day sliding average of five years, and the dashed lines show the total average of five years, with 2009-2013 shown in green and 2050-2054 shown in blue.

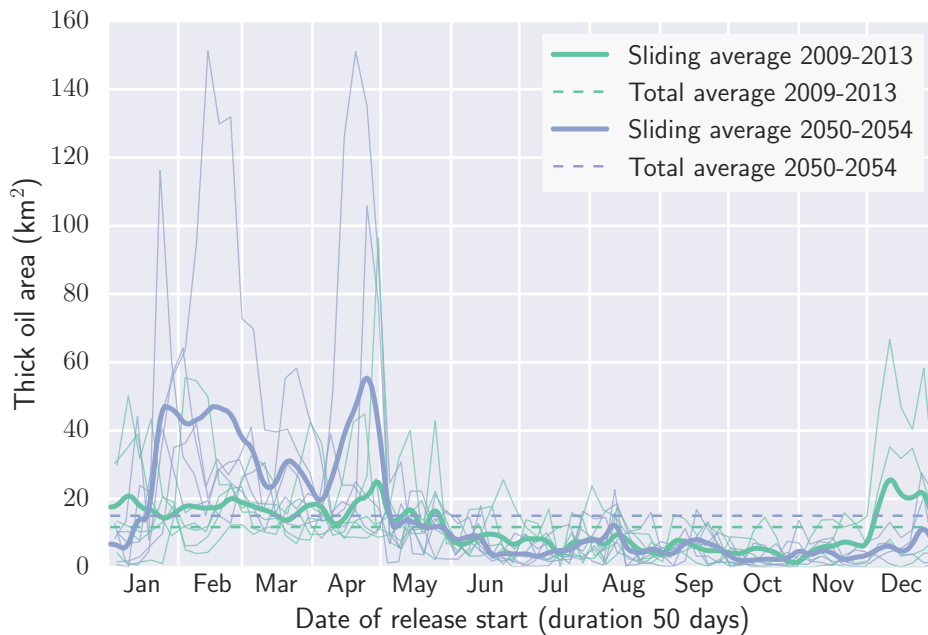


Figure 25: Area (in km<sup>2</sup>) covered by oil thicker than 100 μm, at the end of each 50 day simulation, shown as a function of start date for the simulation. The thin lines show data for the individual years, the thick lines show a five-day sliding average of five years, and the dashed lines show the total average of five years, with 2009-2013 shown in green and 2050-2054 shown in blue.

ends up in the sediment, with an average of around 40% of the total release in the open water season. There is somewhat more oil in the sediments in the future, with an average of 13000

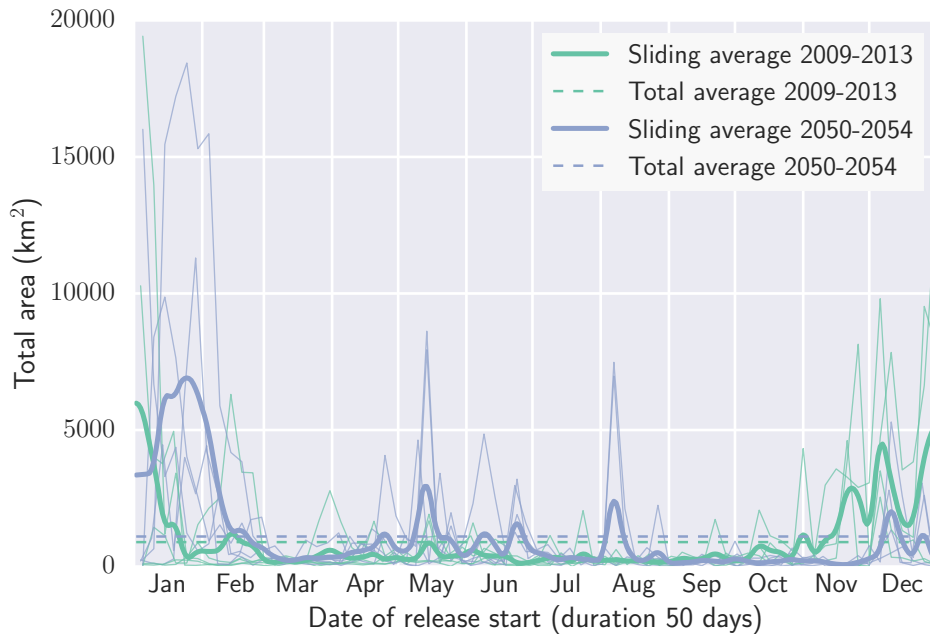


Figure 26: Area (in km<sup>2</sup>) covered by oil, at the end of each 50 day simulation, shown as a function of start date for the simulation. The thin lines show data for the individual years, the thick lines show a five-day sliding average of five years, and the dashed lines show the total average of five years, with 2009-2013 shown in green and 2050-2054 shown in blue.

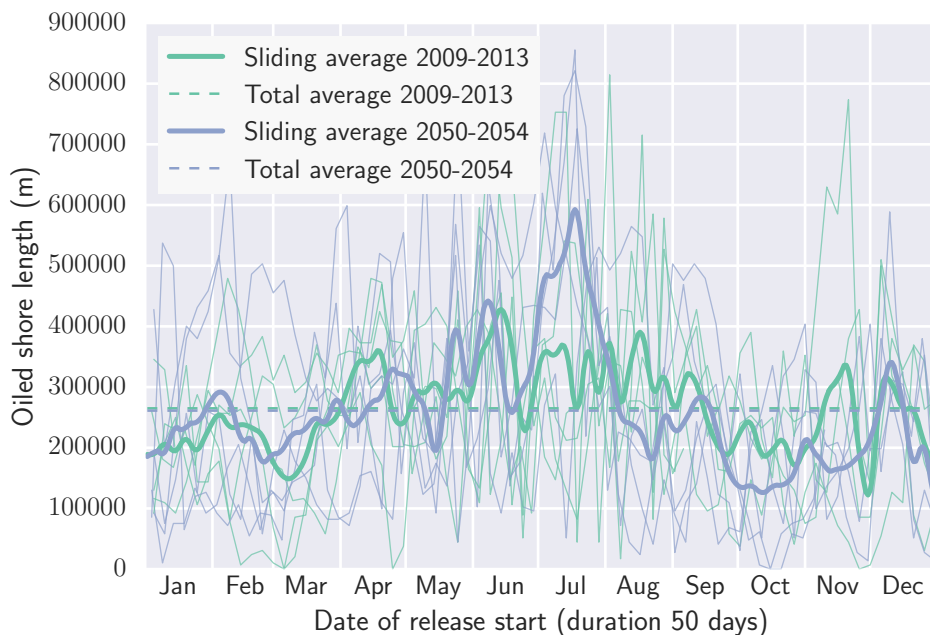


Figure 27: Length (in m) of shore affected by oil, at the end of each 50 day simulation, shown as a function of start date for the simulation. The thin lines show data for the individual years, the thick lines show a five-day sliding average of five years, and the dashed lines show the total average of five years, with 2009-2013 shown in green and 2050-2054 shown in blue.

tons, compared to 11200 tons in the present scenarios. This is out of a total release of 40000 tons.

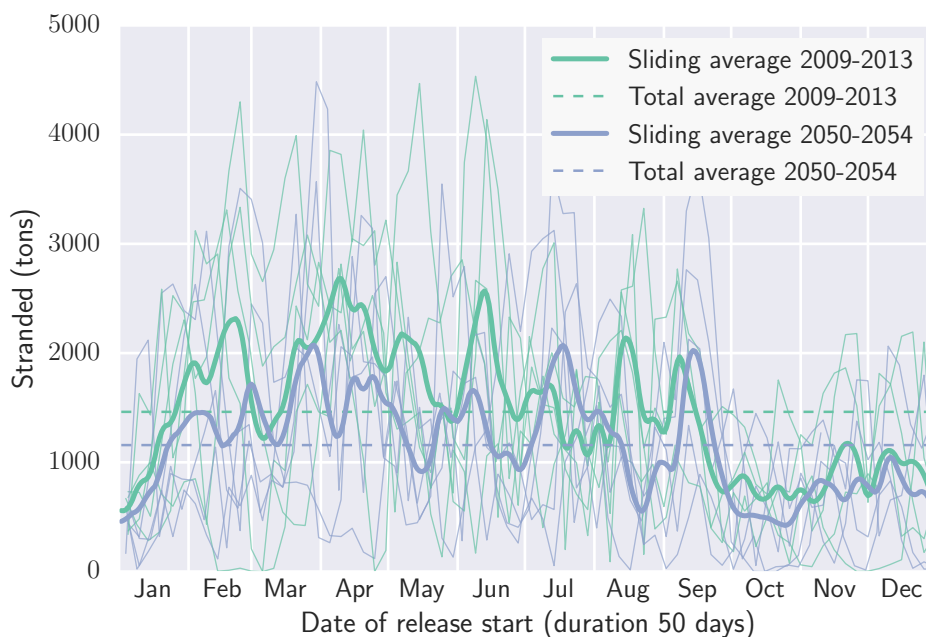


Figure 28: Amount (in metric tons) of oil on the shore, at the end of each 50 day simulation, shown as a function of start date for the simulation. The thin lines show data for the individual years, the thick lines show a five-day sliding average of five years, and the dashed lines show the total average of five years, with 2009-2013 shown in green and 2050-2054 shown in blue.

From Figure 30, which shows the full mass balance, it can be seen that there is a quite significant difference between the winter season with high ice coverage (mainly January to April, see Figure 7, and the summer season. In winter, the bulk of the oil is still trapped under the ice at the end of the 50 day simulations, while in the summer, almost all the oil is either evaporated, biodegraded or deposited in the sediments. It can also be seen that the difference between summer and winter is much larger than the difference between the present and the future scenarios.

All the results that have been presented as time series are also summarised in Table 5.

Figures 31 and 32 show the expectation value and maximum value of oil at the surface respectively. The differences are relatively small, although it can be seen that the surface oil is somewhat more spread out in the future scenarios, especially in Figure 31.

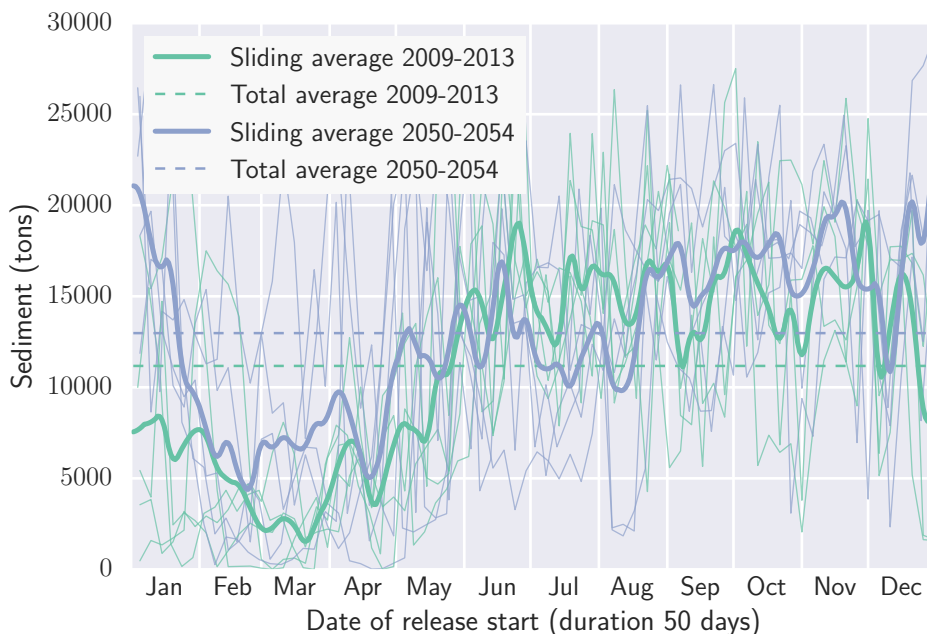


Figure 29: Amount (in metric tons) of oil in the sediments, at the end of each 50 day simulation, shown as a function of start date for the simulation. The thin lines show data for the individual years, the thick lines show a five-day sliding average of five years, and the dashed lines show the total average of five years, with 2009-2013 shown in green and 2050-2054 shown in blue.

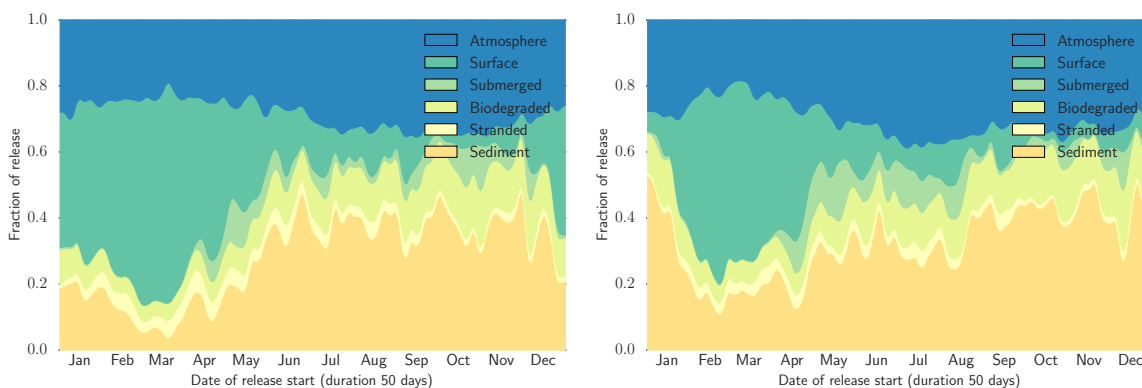


Figure 30: The full mass balance, at the end of each 50 day simulation, as a function of start date for the simulation and shown as a five-day sliding average over the five years. To the left, the years 2009 - 2013, to the right 2050 - 2054.

Table 5: Summary of results for Scenario 2: tanker accident in the Kara Strait.

	Present		Future	
	Average	Standard deviation	Average	Standard deviation
Total area (km <sup>2</sup> )	856	2040	1110	2560
Thick oil area (km <sup>2</sup> )	11.9	11.9	15.3	23.1
Oiled shore length (m)	267000	150000	262000	173000
Sediment (tons)	11000	7170	12900	7280
Stranded (tons)	1500	998	1170	895
Biodegraded (tons)	4020	1750	4510	1630
Submerged (tons)	1490	2530	1990	3240
Surface (tons)	10600	9350	7390	8180
Atmosphere (tons)	11400	2560	12100	2860

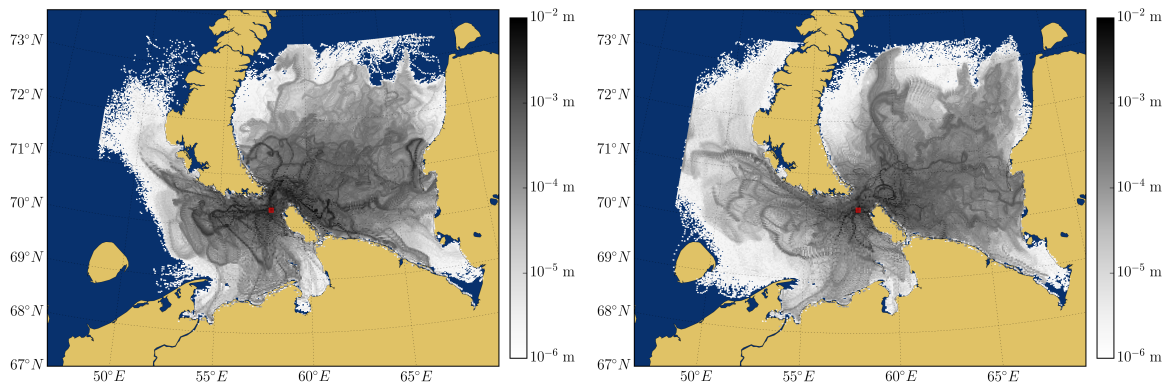


Figure 31: Maximum value of oil thickness on surface, over all simulations over the two five year periods. To the left 2009 - 2013, to the right 2050 - 2054. Only values larger than  $10^{-6}$  m is shown.

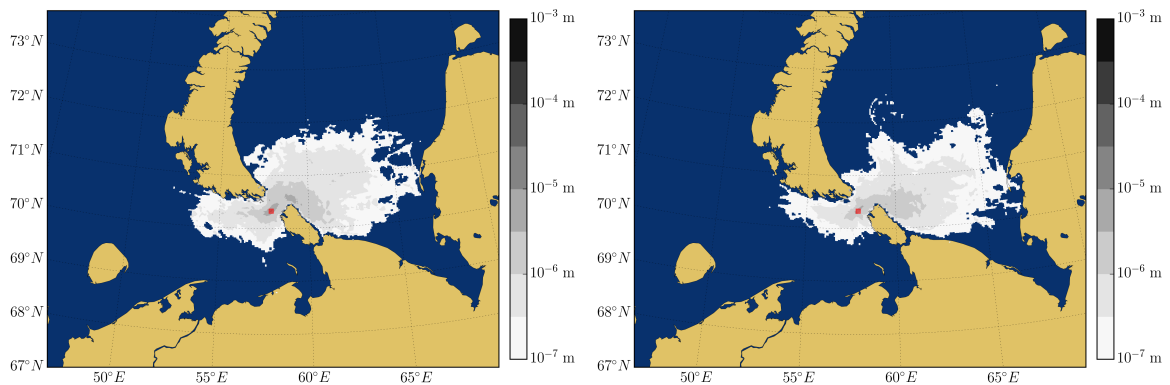


Figure 32: Expectation value of oil thickness on surface, over all simulations over the two five year periods. To the left 2009 - 2013, to the right 2050 - 2054. Only values larger than  $10^{-7}$  m is shown.

### 4.3 Scenario 3: Pipeline Rupture

As for Scenario 2 (shipping accident), many of the same observations that were made about the results of Scenario 1 (the well blowout) will apply to Scenario 3 as well. Hence, the discussion here will be somewhat shorter, with more detailed comments where the results differ from what was seen previously.

In Figure 33, the amount of oil on the surface, at the end of each 50 day simulation, is shown as a function of start date of that simulation. The general trend of less oil on the surface in summer is visible, with hardly any oil on the surface during the period from June to November for either scenario. The present scenarios show somewhat more oil on the surface on average, with 34 tons, compared to 25 tons for the future.

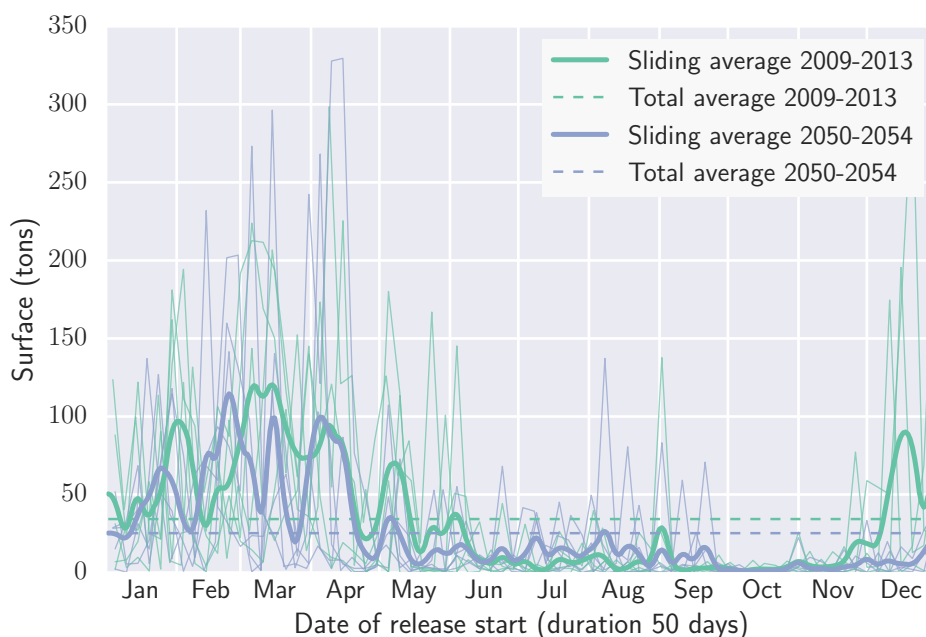


Figure 33: Amount (in metric tons) of oil on the surface, at the end of each 50 day simulation, shown as a function of start date for the simulation. The thin lines show data for the individual years, the thick lines show a five-day sliding average of five years, and the dashed lines show the total average of five years, with 2009-2013 shown in green and 2050-2054 shown in blue.

The area covered by oil thicker than  $100\ \mu\text{m}$ , and the total area covered by oil are shown in Figures 34 and 35 respectively. As this is a much smaller release, the area covered by oil thicker than  $100\ \mu\text{m}$  is much smaller than in the two other scenarios. Still, the trend of larger area covered in the winter is visible here as well. The differences in the total averages are quite small:  $0.084\ \text{km}^2$  (area with thick oil) and  $15\ \text{km}^2$  (total area) for the present scenarios, versus  $0.074\ \text{km}^2$  (area with thick oil) and  $19\ \text{km}^2$  (total area) for the future scenarios.

As for Scenario 2, it can be seen from the thin lines showing the individual years in Figure 34 that in some cases the area covered by thick oil can reach much higher values than the average, the maximum for the future scenarios being  $3\ \text{km}^2$ , or 40 times the average.

Figure 36 shows the length of oiled shoreline, and Figure 37 shows the amount of oil on the shore. The length of oiled shoreline is in this case larger in the present scenarios than in the future, at 25 km and 21 km respectively. Amount of oil on the shore shows a similar difference, with 35 tons at present, compared to 27 tons in the future scenarios. Note that compared to

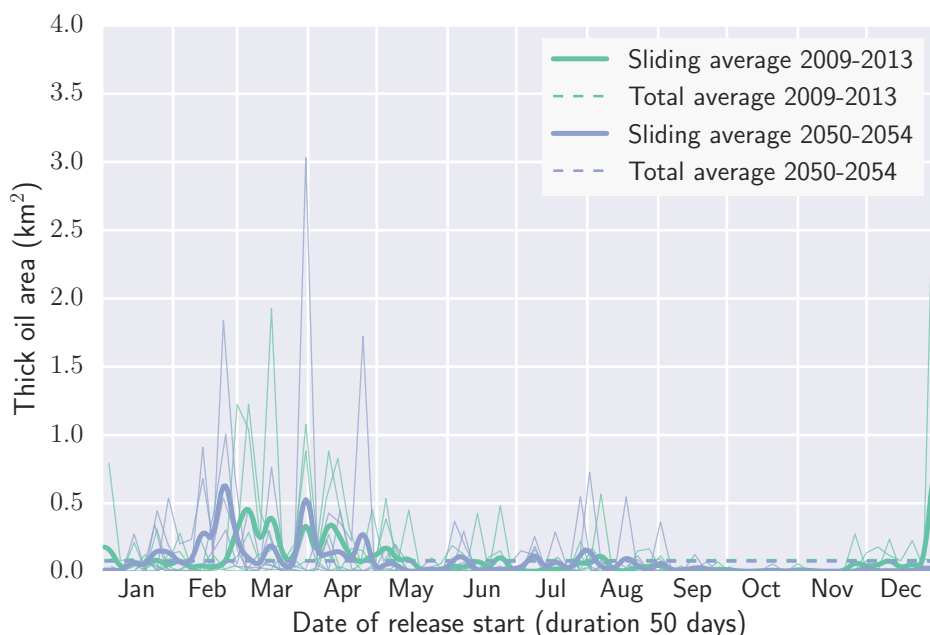


Figure 34: Area (in km<sup>2</sup>) covered by oil thicker than 100 μm, at the end of each 50 day simulation, shown as a function of start date for the simulation. The thin lines show data for the individual years, the thick lines show a five-day sliding average of five years, and the dashed lines show the total average of five years, with 2009-2013 shown in green and 2050-2054 shown in blue.

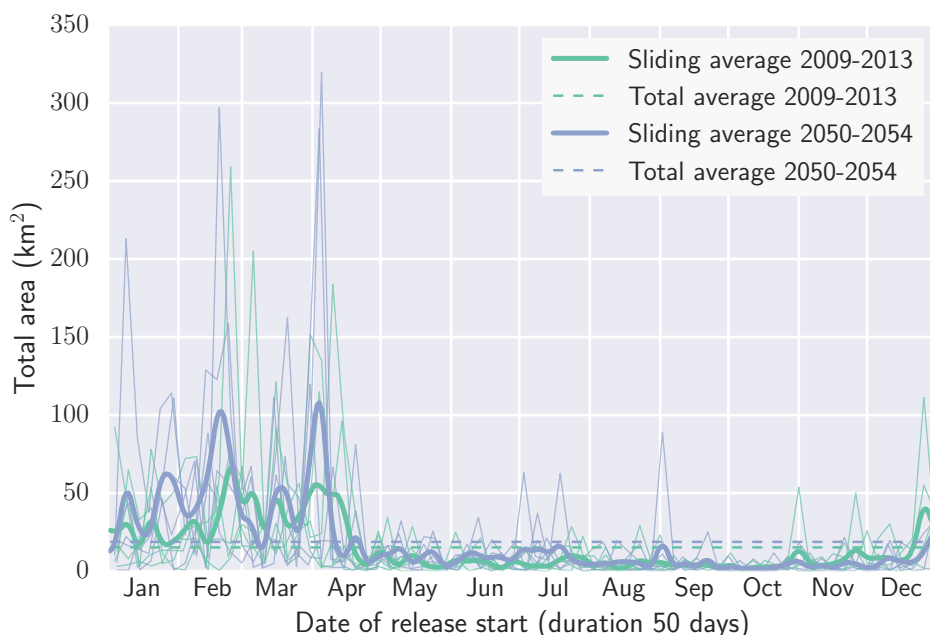


Figure 35: Area (in km<sup>2</sup>) covered by oil, at the end of each 50 day simulation, shown as a function of start date for the simulation. The thin lines show data for the individual years, the thick lines show a five-day sliding average of five years, and the dashed lines show the total average of five years, with 2009-2013 shown in green and 2050-2054 shown in blue.

Scenario 1 (well blowout), this release occurs much closer to land, and in an open bay. Since ice generally prevents transport and spreading, the ice could potentially trap the oil closer to land,

leading to more beaching, while in Scenario 1 the ice served to partially protect the shoreline.

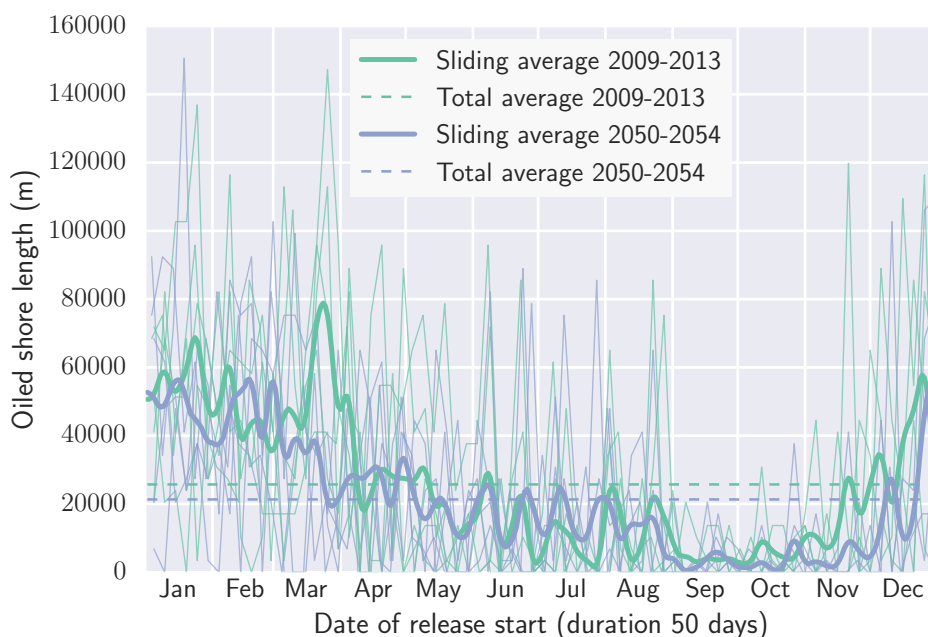


Figure 36: Length (in m) of shore affected by oil, at the end of each 50 day simulation, shown as a function of start date for the simulation. The thin lines show data for the individual years, the thick lines show a five-day sliding average of five years, and the dashed lines show the total average of five years, with 2009-2013 shown in green and 2050-2054 shown in blue.

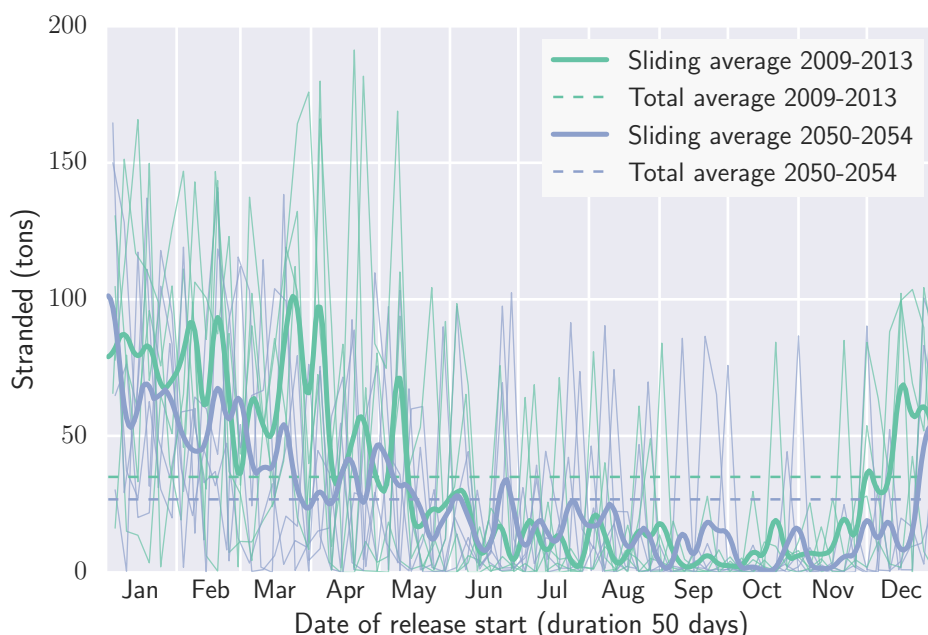


Figure 37: Amount (in metric tons) of oil on the shore, at the end of each 50 day simulation, shown as a function of start date for the simulation. The thin lines show data for the individual years, the thick lines show a five-day sliding average of five years, and the dashed lines show the total average of five years, with 2009-2013 shown in green and 2050-2054 shown in blue.

The amount of oil in the sediments is shown in Figure 38, and as in Scenario 2 a fairly strong

anti-correlation with ice coverage (shown in Figure 9) is observed, i.e., when there is high ice cover, less oil ends up in the sediments. Even more so than in Scenario 2, the area is quite shallow, with large areas at only around 20 meters deep, and hence a significant fraction of the release ends up in the sediment. However, the difference between the present and the future scenarios is modest, with 170 tons and 177 tons respectively.

From Figure 39, which shows the full mass balance, a significant difference between the winter and the summer season is observed, although it is less pronounced than what was the case for Scenario 2. While winter shows less oil in the sediments and more on the surface (note that surface includes oil trapped under the ice), another strong trend is that winter is more variable, while summer shows a relatively constant mass balance. Again, it can be seen that the difference between summer and winter is much larger than the difference between the present and the future scenarios.

All the results that have been presented as time series are also summarised in Table 6.

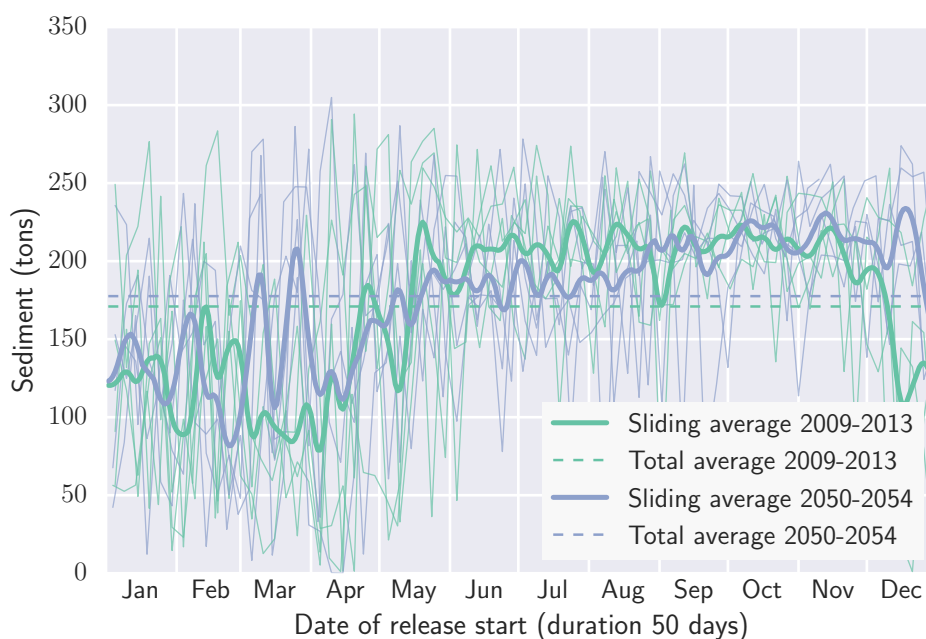


Figure 38: Amount (in metric tons) of oil in the sediments, at the end of each 50 day simulation, shown as a function of start date for the simulation. The thin lines show data for the individual years, the thick lines show a five-day sliding average of five years, and the dashed lines show the total average of five years, with 2009-2013 shown in green and 2050-2054 shown in blue.

Figures 40 and 41 show the expectation value and maximum value of oil at the surface respectively. The differences in expectation values are hardly visible, while Figure 40 shows that in the future scenarios the oil in some cases reach further north along the western coast of Novaya Zemlya, and the north eastern coast of Kolguyev Island.

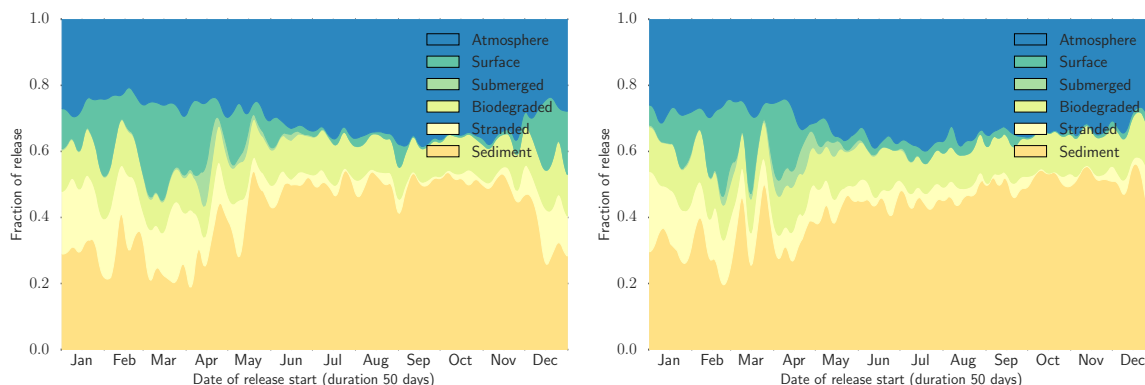


Figure 39: The full mass balance, at the end of each 50 day simulation, as a function of start date for the simulation and shown as a five-day sliding average over the five years. To the left, the years 2009 - 2013, to the right 2050 - 2054.

Table 6: Summary of results for Scenario 3: pipeline rupture near Varandey.

	Present		Future	
	Average	Standard deviation	Average	Standard deviation
Total area (km <sup>2</sup> )	15.7	29.3	19.1	38.4
Thick oil area (km <sup>2</sup> )	0.0879	0.274	0.0758	0.247
Oiled shore length (m)	26300	31700	21500	27400
Sediment (tons)	169	74.3	177	64.3
Stranded (tons)	35.9	45.8	27.0	35.9
Biodegraded (tons)	46.6	11.5	48.4	11.8
Submerged (tons)	3.39	17.0	4.07	15.2
Surface (tons)	35.4	56.5	25.7	49.1
Atmosphere (tons)	125	28.7	134	28.6

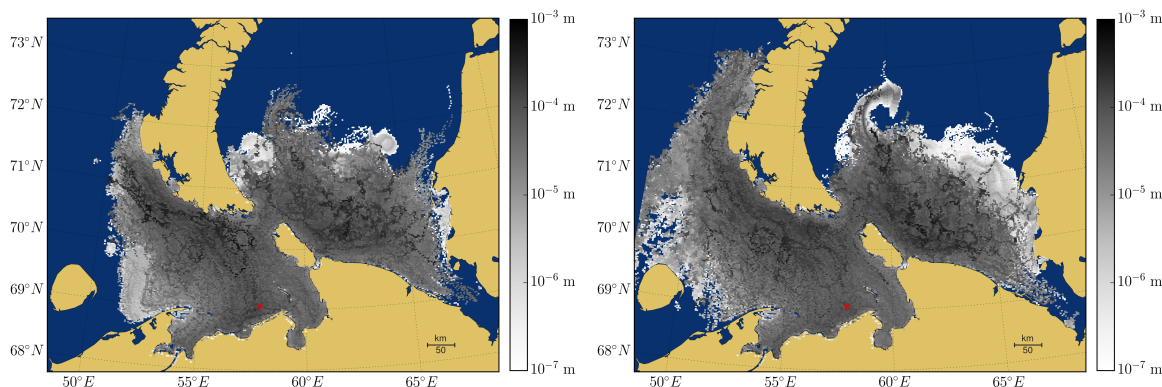


Figure 40: Maximum value of oil thickness on surface, over all simulations over the two five year periods. To the left 2009 - 2013, to the right 2050 - 2054. Only values larger than 10<sup>-7</sup> m is shown.

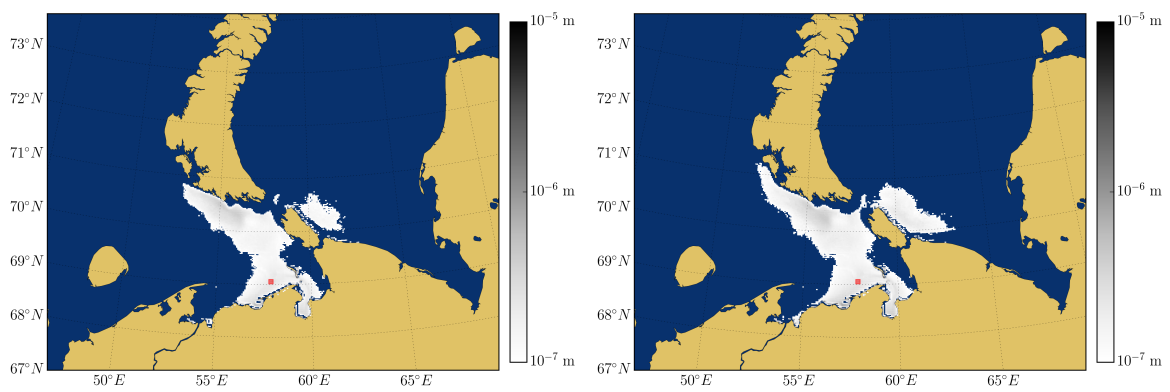


Figure 41: Expectation value of oil thickness on surface, over all simulations over the two five year periods. To the left 2009 - 2013, to the right 2050 - 2054. Only values larger than  $10^{-7}$  m is shown.

## 5 Conclusions

The conclusion from the case studies is that the same trend can be observed in all three scenarios: During periods with low ice coverage, there is in general more spreading and a less concentrated surface slick. For individual years, this can be seen as more spreading in summer than in winter, and for the full ensemble of simulations, there is on average more spreading in the future scenarios than in the present. However, for almost all of the endpoints considered here, such as amount of oil on the surface and length of oiled shoreline, the variation between summer and winter is larger than the variation between the present and the future. A notable exception is the amount of oil in the sediment in Scenario 1 (shown in Figure 20), which shows a significant increase in the future scenarios, presumably due to the combination of more open water and possibly stronger winds leading to a deeper mixed layer.

The difference in spreading has implications for consequences of a spill, as well as response options. More spreading means larger affected area, but also lower average concentrations over that area. It is also easier to respond to a thicker surface slick, however the presence of ice may limit the available response options.

When crude oil is spilled at sea, a number of natural processes occur that change the physical and chemical properties of the oil. In ice-covered waters this time-dependent weathering can be significantly reduced, depending on ice type, ice coverage and energy conditions. This can be an advantage and contribute to the enhancement of response effectiveness for certain oil spill scenarios. The window of opportunity for *in situ* burning and the use of dispersant operations in ice-covered waters can in some cases increase significantly compared with an open-water scenario. Both techniques were tested as part of the Oil in Ice JIP conducted by SINTEF during 2006-2009, and found to be feasible for response to oil in ice [20].

The probability of oil spill accidents in the Arctic is expected to increase in concert with increases in transport and resource exploration and extraction activities. The results reported here suggest that future oil spills in a warming climate will result in greater areal coverage and shoreline exposure, due to reduced ice coverage. These two considerations point towards a significant increase in environmental risk, defined as the probability of an event, in this case an oil spill, weighted by the magnitude of the resulting environmental injury. A comparative environmental risk assessment would therefore be a natural follow-on to the present study.

Ensemble simulations, such as those performed in this study, make up an important part of planning by allowing us to study a range of possible outcomes. They can also be used operationally, for longer term prediction of oil trajectories, outside of normal forecast ranges, as was done, for example, during the Deepwater Horizon [21]. However, modelling the interactions of oil and ice, and especially modelling oil spill response in ice covered waters, are topics that need more research.

Eisenhower supposedly said

“ In preparing for battle, I have always found that plans are useless, but planning is indispensable. ”

Whether or not he actually said it, it is true that planning is of the utmost importance in preparation for an Arctic oil spill, and we believe ensemble simulations to be an essential tool during planning. In the future, with on average larger footprint from an Arctic oil spill, and also higher variance in many endpoints, statistical information on likely outcomes of a spill will be even more important.

## References

- [1] Øistein Johansen. Deepblow – a lagrangian plume model for deep water blowouts. *Spill Science & Technology Bulletin*, 6(2):103 – 111, 2000.
- [2] Øistein Johansen, Henrik Rye, and Cortis Cooper. Deepspill—field study of a simulated oil and gas blowout in deep water. *Spill Science & Technology Bulletin*, 8(5–6):433 – 443, 2003.
- [3] Per Johan Brandvik, Øistein Johansen, Frode Leirvik, Umer Farooq, and Per S. Daling. Droplet breakup in subsurface oil releases – part 1: Experimental study of droplet breakup and effectiveness of dispersant injection. *Marine Pollution Bulletin*, 73(1):319 – 326, 2013.
- [4] Øistein Johansen, Per Johan Brandvik, and Umer Farooq. Droplet breakup in subsea oil releases – part 2: Predictions of droplet size distributions with and without injection of chemical dispersants. *Marine Pollution Bulletin*, 73(1):327 – 335, 2013.
- [5] M Reed, PS Daling, OG Brakstad, I Singsaas, LG Faksness, B Hetland, and N Ekrol. Oscar 2000: A multi-component 3-dimensional oil spill contingency and response model. pages 663–680, 2000.
- [6] A Drozdowski, S Nudds, CG Hannah, H Niu, I Peterson, and W. Perrie. Review of oil spill trajectory modelling in the presence of ice. *Canadian Technical Report of Hydrographic and Ocean Sciences*, 274, 2011.
- [7] WD Hibler III. A dynamic thermodynamic sea ice model. *Journal of Physical Oceanography*, 9(4):815–846, 1979.
- [8] Dag Slagstad and Thomas A. McClimans. Modeling the ecosystem dynamics of the barents sea including the marginal ice zone: I. physical and chemical oceanography. *Journal of Marine Systems*, 58(1–2):1 – 18, 2005.
- [9] James F Price, Robert A Weller, and Robert Pinkel. Diurnal cycling: Observations and models of the upper ocean response to diurnal heating, cooling, and wind mixing. *Journal of Geophysical Research: Oceans (1978–2012)*, 91(C7):8411–8427, 1986.
- [10] Joseph Smagorinsky. General circulation experiments with the primitive equations: I. the basic experiment\*. *Monthly weather review*, 91(3):99–164, 1963.
- [11] EC Hunke and JK Dukowicz. An elastic-viscous-plastic model for sea ice dynamics. *Journal of Physical Oceanography*, 27(9):1849–1867, 1997.
- [12] <http://volkov.oce.orst.edu/tides/global.html>.
- [13] DP Dee, SM Uppala, AJ Simmons, P Berrisford, P Poli, S Kobayashi, U Andrae, MA Balmaseda, G Balsamo, P Bauer, et al. The era-interim reanalysis: Configuration and performance of the data assimilation system. *Quarterly Journal of the Royal Meteorological Society*, 137(656):553–597, 2011.
- [14] Elke Keup-Thiel, Holger Göttel, and Daniela Jacob. Regional climate simulations for the barents sea region. *Boreal environment research*, 11(5):329–339, 2006.

- [15] M.R. McNutt, G. Camilli, P. Guthrie, V. Hsieh, B. Labson, D. Lehr, A. Maclay, Ratzel, and M. Sogge. Assessment of flow rate estimates for the deepwater horizon / macondo well oil spill. Technical report, 2011.
- [16] James W Hurrell. Decadal trends in the north atlantic oscillation: regional temperatures and precipitation. *Science*, 269(5224):676–679, 1995.
- [17] RR Dickson, TJ Osborn, JW Hurrell, J Meincke, J Blindheim, B Adlandsvik, T Vinje, G Alekseev, and W Maslowski. The arctic ocean response to the north atlantic oscillation. *Journal of Climate*, 13(15):2671–2696, 2000.
- [18] James W Hurrell and Harry Van Loon. Decadal variations in climate associated with the north atlantic oscillation. In *Climatic Change at High Elevation Sites*, pages 69–94. Springer, 1997.
- [19] Tim Woollings, Jonathan M Gregory, Joaquim G Pinto, Mark Meyers, and David J Brayshaw. Response of the north atlantic storm track to climate change shaped by ocean-atmosphere coupling. *Nature Geoscience*, 5(5):313–317, 2012.
- [20] Stein Erik Sørstrøm, Per Johan Brandvik, Ian Buist, Per Daling, David Dickins, Liv-Guri Faksness, Steve Potter, Janne Fritt-Rasmussen, and Ivar Singsaas. Joint industry program on oil spill contingency for arctic and ice-covered waters: Summary report. Technical report, SINTEF, 2010.
- [21] CHCH Barker. A statistical outlook for the deepwater horizon oil spill. *Monitoring and Modeling the Deepwater Horizon Oil Spill: A Record-Breaking Enterprise*, pages 237–244, 2011.